制动帆可控的立方星设计与验证

Design and Verification of CubeStar with Controllable Brake Sail

设计报告

Design report

学生姓名 陈铮、熊梓岑、景思源
Student's name Chen Zheng, Xiong Zicen, Jing Siyuan

指导老师 韩潮
Instructor Han Chao

培养院系 宇航学院
Training department School of Astronautics

2021.06

目 录

Catalog

1 绪论
Introduction

1.1 研究背景和意义
Research background and significance

随着商业航天的蓬勃发展,近几年进入轨道的卫星,特别是低轨小卫星,已呈爆发式增长。按照国防科工局《空间碎片减缓与防护管理办法》等文件要求, 低轨卫星应具备主动离轨能力。目前,低轨、体积小的卫星常采用非推进式离轨方式， 利用高空稀薄大气、地球磁场、太阳光压等阻力进行离轨制动的技术已有广泛的研究和应用。

With the rapid development of commercial spaceflight, the number of satellites in orbit, especially small satellites in low orbit, has increased explosively in recent years. According to the requirements of documents such as "Space Debris Mitigation and Protection Management Measures" issued by the National Defense Science and Technology Bureau, LEO satellites should have the ability of active de-orbit. At present, low-orbit and small-size satellites often use non-propulsion deorbit mode, and the deorbit braking technology has been widely studied and applied by using the resistance of high altitude rarefied atmosphere, earth magnetic field, solar light pressure and so on.

常见返回式航天器是通过制动（反推）火箭从原运行轨道脱离，再利用降落伞和回收系统在大气层较低高度减速并着陆。运载火箭子级回收可以分为伞降回收、带翼飞回式和垂直返回回收三种类型。伞降回收是利用降落伞减速，通过姿控发动机（Reaction Control System，RCS）或者翼伞来调整姿态。带翼飞回式子级回收的主要思想是在传统火箭上添加机翼，利用控制舵面和 RCS 系统，实现水平着陆。火箭子级垂直回收是火箭子级在完成任务后，通过自身携带的控制系统和动力装置，按照设定的轨迹自主飞回，并以垂直的箭体姿态缓慢降落到指定着陆场。[1]

Common recoverable spacecraft are released from the original orbit by braking (thrust reverser) rockets, and then decelerated and landed at lower altitudes in the atmosphere by parachutes and recovery systems. Launch vehicle substage recovery can be divided into three types: parachute recovery, winged flyback and vertical return recovery. Parachute recovery is the use of parachute deceleration, and the attitude is adjusted by Reaction Control System (RCS) or parafoil. The main idea of winged flyback substage recovery is to add wings to the traditional rocket and use the control surface and RCS system to achieve horizontal landing. Vertical recovery of rocket sub-stage is that after completing the task, the rocket sub-stage flies back autonomously according to the set trajectory through its own control system and power device, and slowly lands to the designated landing site in a vertical attitude.[1]

以上航天器离轨再入的方式所需的制动设备较为复杂、成本高，且需要携带一定质量的推进剂，机动距离受所携带燃料的约束。因此，我们可以尝试将制动帆离轨技术应用于近地轨道的返回式卫星或需要回收的空间站等。通过控制卫星制动帆的迎风面积，改变卫星在运行速度方向的阻力，逐渐降低轨道，以此控制或者精确预报卫星轨道改变，最终使卫星落点在预定区域。此方法可以采用成本低、结构简单的 CubeSat 立方星作可行性验证。

The braking equipment required by the above reentry modes of spacecraft is complex and costly, and it needs to carry a certain mass of propellant, and the maneuvering distance is constrained by the fuel carried. Therefore, we can try to apply the brake sail de-orbit technology to the recoverable satellite in low earth orbit or the space station that needs to be recovered. By controlling the windward area of the brake sail of the satellite, the resistance of the satellite in the running speed direction is changed, and the orbit is gradually lowered, so that the change of the orbit of the satellite is controlled or accurately predicted, and finally the landing point of the satellite is in a predetermined area. The feasibility of this method can be verified by CubeSat with low cost and simple structure.

1.2 离轨技术研究现状
Research Status of Deorbit Technology

1.2.1 气动离轨
Pneumatic deorbit

气动离轨技术是一项适用于 LEO 区域任务后航天器离轨的新技术，借助近地轨道区域的高空稀薄大气阻力，使完成了特定任务或失效的航天器降低轨道高度，最终进入稠密大气层。常用气动离轨方式如下：

Aerodynamic deorbiting technology is a new technology for spacecraft deorbiting after a mission in the LEO region. With the help of the drag of the rarefied atmosphere at high altitude in the low earth orbit region, the spacecraft that has completed a specific mission or has failed will lower its orbit altitude and eventually enter the dense atmosphere. The common methods of pneumatic deorbit are as follows:

（1） 薄膜离轨方式。利用充气装置形成气球、抛物面等形状，提高卫星在低地球轨道上的气动力，迫使卫星提早离轨。但需要携带气体增压装置，会给卫星发射和长时间在轨飞行带来了一定的安全隐患。[2]

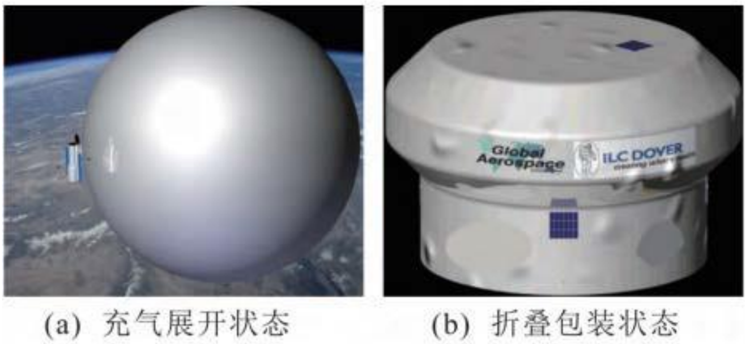

Film off-track mode. Inflatable devices are used to form balloons, paraboloids and other shapes to improve the aerodynamic force of satellites in low earth orbit and force satellites to leave orbit earlier. However, the need to carry a gas pressurization device will bring some potential safety hazards to satellite launching and long-term on-orbit flight.[2]

图1.1 薄膜轨道衰降装置（GOLD）
Film Track Degradation Device (GOLD)

此外，还有一种充气式薄膜离轨方式。在立方体卫星寿命结束时，充气式离轨装置启动工作，从结构容腔内弹出并展开一个金字塔形离轨装置，支撑管充气后，将刚化材料夹在支撑管两层薄膜材料之间实现刚化，以增加柔性展开结构的刚度。[3]

In addition, there is an inflatable membrane off-track mode. At the end of the service life of the CubeSat, the inflatable de-orbit device is started to work, and a pyramid-shaped de-orbit device is ejected from the structure cavity and unfolded; after the support tube is inflated, the rigidizing material is clamped between two layers of film materials of the support tube to realize rigidization, so as to increase the rigidity of the flexible unfolding structure.[3]

图1.2 展开后的充气式薄膜离轨装置
Inflatable film off-track device after being unfolded

（2） 制动帆离轨方式。制动帆离轨是通过弹出杆状支架来展开帆状薄膜，增大卫星移动方向上的阻力，使卫星减速最终达到离轨的目的。制动帆离轨装置具有质量轻、结构紧凑的

特点。[1]

Brake sail off-track mode. Brake sail deorbit is to deploy the sail-like film by popping up the rod-like bracket, increase the resistance in the direction of satellite movement, and slow down the satellite to achieve the ultimate purpose of deorbit. The brake sail off-track device has the characteristics of light weight and compact structure.[1]

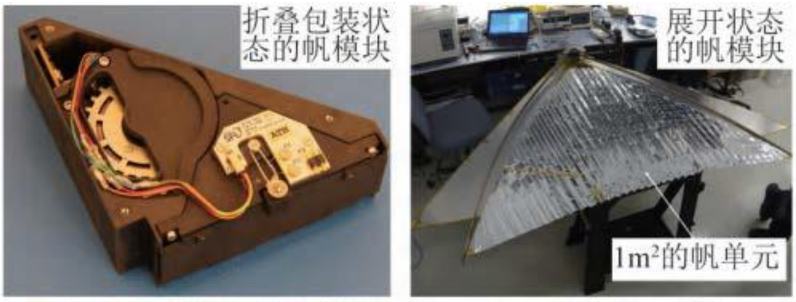

(a) 折叠包装状态的帆模块　(b) 展开状态的阻力帆

图1.3 阻力帆离轨装置

Device for preventing Lifan from leaving the track

1.2.2 绳系离轨

The rope is off the track

绳系离轨原理：电动力系绳是由一根长度很长、质量很小的导线构成，一段连接于航天器上另一端连接一重物。航天器带着系绳一起沿轨道运动，在运动过程中不断切割地球磁场的磁力线，在系绳两端产生电动势，因而又受到地磁场的阻力，使整个系统的运行速度逐渐变小，轨道高度不断降低，直至脱离轨道，再入大气层。

Rope tether de-orbit principle: The electrodynamic tether is composed of a wire with a long length and a small mass, one end of which is connected to the spacecraft and the other end is connected to a heavy object. The spacecraft with the tether moves along the orbit. In the process of moving, it continuously cuts the magnetic lines of the earth's magnetic field and generates electromotive force at both ends of the tether. Therefore, it is subject to the resistance of the earth's magnetic field, so that the speed of the whole system gradually decreases, and the orbit altitude decreases continuously until it leaves the orbit and re-enters the atmosphere.

1.2.3 太阳帆推移离轨

The solar sail moves out of orbit

太阳帆推移离轨依靠太阳光光子对帆的不断撞击从而使太阳帆动量不断增加，从而产生足够的加速度。太阳光子产生的推力方向和太阳帆的速度方向相反，使太阳帆减速变轨到更低的轨道上。

The solar sail is pushed out of orbit by the continuous impact of solar photons on the sail, so that the momentum of the solar sail is continuously increased, thereby generating sufficient acceleration. The direction of thrust generated by solar photons is opposite to the speed of the solar sail, which makes the solar sail slow down and change orbit to a lower orbit.

1.2.4 喷气变轨

Jet orbit transfer

目前应用最为成熟的是采用喷气变轨的方法进行返回离轨。采用推进剂或气瓶，喷气产生推力离轨，进行离轨机动，使卫星脱离原来的工作轨道进入一个短寿命轨道，在大气阻力的作用下落入稠密大气层烧毁。但这种方式成本高、质量大，不适用于小型卫星。

At present, the most mature application is to use the method of jet orbit transfer to return to the orbit. Propellant or gas cylinders are used to generate thrust for de-orbit, and de-orbit maneuvers are carried out to make the satellite leave the original working orbit and enter a short-lived orbit, which falls into the dense atmosphere and burns up under the action of atmospheric drag. However, this method is not suitable for small satellites because of its high cost and high mass.

1.3 制动帆应用研究现状

Application and Research Status of Brake Sail

对地探测任务的增加使得立方星发射数量飞速上升，加上立方星寿命相对较短，报废立方星会成为太空碎片或垃圾，威胁地球近地轨道上的其他航天器。因此在立方星技术发展比较成熟的基础上，国内外研究机构对制动帆装置在立方星上的应用展开了进一步研究。

The increase of earth exploration missions has led to a rapid increase in the number of cubic satellites launched, coupled with the relatively short life of cubic satellites, abandoned cubic satellites will become space debris or garbage, threatening other spacecraft in low earth orbit. Therefore, on the basis of the mature development of CubeSat technology, domestic and foreign research institutions have carried out further research on the application of brake sail device on CubeSat.

Cubesail 制动帆装置采用四根弹簧桅杆展开帆薄膜，桅杆的设计具有特色，

The Cubesail brake sail device uses four spring masts to deploy the sail membrane, and the design of the mast has its own characteristics.

通过两根“（”形桅杆拼接成一根柱面桅杆，改善了桅杆凹凸两面弯曲扭矩不同带来的帆面姿态变化。[4]

Two ″（″ shaped masts are spliced to form a cylindrical mast, which improves the sail surface attitude change caused by the different bending torques on the concave and convex sides of the mast.[4]

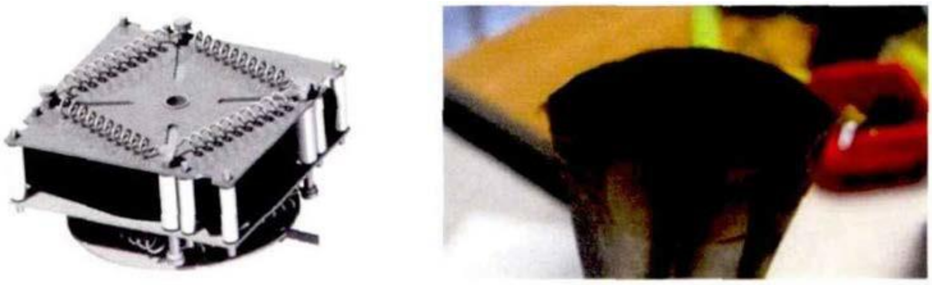

(a)展开机构图　　　　(b)桅杆截面

图1.4 CubeSail 展开机构和桅杆截面图

CubeSail Deployment Mechanism and Mast Section

Gossamer Deorbit 制动帆装置[5]帆材料为双面镀铝的 Kapton，帆绕中心轴缠绕裹紧，保存在帆仓中。该设计引入三阶可伸缩套管的应用，通过压缩弹簧恢复自由状态带动可伸缩套管伸长，能够将展开机构弹出到距离卫星主体 0.6m 远处，目的是让卫星的质心远离帆，更好地保证帆的迎风面积达到最大，减少离轨时间。

Gossamer Deorbit Brake Sail Device[5]The sail material is double-sided aluminized

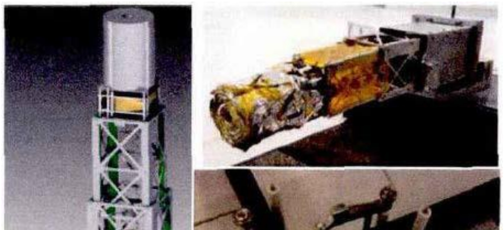

Kapton, which is wrapped around the central axis and stored in the sail compartment. The design introduces the application of the three-order telescopic sleeve. By restoring the free state of the compression spring to drive the telescopic sleeve to extend, the deployment mechanism can be ejected to a distance of 0. 6m from the main body of the satellite, so as to make the center of mass of the satellite far away from the sail, better ensure that the windward area of the sail reaches the maximum, and reduce the deorbit time.

图1.5 三阶可伸缩套管图

3rd Order Retractable Casing Drawing

InflateSail 立方星[6]通过四根桅杆展开带动帆的打开，桅杆和帆薄膜分开存储。四根桅杆选用碳纤维复合材料，缠绕在中心轴上，通过中心轴安装的电机驱动弹出。展开机构和卫星之间放置有

一根可充气的支撑柱，制动帆展开时，可充气支撑柱充气伸长，长度达到 1m，使制动帆远离卫星，增大迎风面积。

The InflateSail CubeStar[6]opens the sail by deploying four masts, which are stored separately from the sail membrane. The four masts are made of carbon fiber composite materials, which are wound on the central shaft and ejected by the motor installed on the central shaft. An inflatable support column is arranged between the unfolding mechanism and the satellite, and when the brake sail is unfolded, the inflatable support column is inflated and stretched to be 1m long, so that the brake sail is far away from the satellite, and the windward area is increased.

CANX-7 立方星卫星[7]由 4 个相同的体形制动帆组成，可以实现 3 种不同质

The CANX-7 CubeSat[7]consists of four identical body brake sails, which can realize three different masses.

量大小的低地球轨道卫星在 25 年内脱离轨道。该装置通过模块化设计使其能够适应多种质量的立方星平台，可根据卫星的重量和轨道高度选择帆单元的数量，

A large number of low Earth orbit satellites will be de-orbited within 25 years. Through modular design, the device can adapt to cubic star platforms with various masses, and the number of sail units can be selected according to the weight and orbit height of the satellite.

调整帆的阻力面积。
Adjust the drag area of the sail.

LightSail-1 通过四根 4m 的桅杆展开四个三角形帆，帆完全展开后呈正方形。桅杆选用 TRAC 结构，便于折叠缠绕，具有较高的比强度，缠绕后能通过自身储存的机械能弹出。帆和桅杆分开存储，帆和桅杆之间通过拉簧连接。[8]

LightSail-1 deploys four triangular sails through four 4m masts, and the sails are square when fully deployed. The mast adopts TRAC structure, which is easy to fold and wind, has high specific strength, and can be ejected by its own stored mechanical energy after winding. The sail and the mast are stored separately, and the sail and the mast are connected by a tension spring.[8]

“南理工三号”立方体卫星[9]用四个直角三角形薄膜帆组合成正方形的制动帆，每个三角形薄膜帆的三个顶角分别固定，减小抖动增加可靠性。该装置采用单中心展开方案，收拢时，四根弹性桅杆都缠绕在展开装置中心轴上；展开时，四根弹性桅杆从展开装置的四个顶角处弹出带动制动帆并为制动帆提供支撑。

"Nanjing University of Technology 3" CubeSat[9] uses four right-angled triangular membrane sails to form a square braking sail, and the three vertex angles of each triangular membrane sail are fixed respectively to reduce jitter and increase reliability. The device adopts a single-center unfolding scheme, and four elastic masts are wound on a central shaft of the unfolding device when the device is folded; When deployed, the four elastic masts spring out from the four top corners of the deployment device to drive the brake sail and provide support for the brake sail.

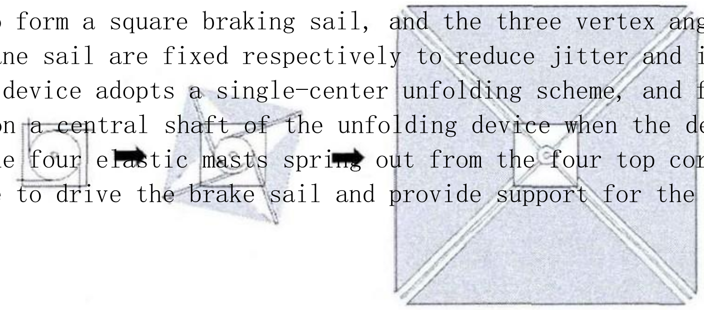

图1.6 "南理工三号"立方星制动离轨装置展开过程
Deployment process of "Nanjing University of Science and Technology No.3" cubic star braking deorbit device

“恩来一号”教育卫星采用混合存储式设计的方案，分为展开机构，存储机构和锁紧机构三个主要部分，采用“（”型弹簧桅杆，制动帆薄膜折叠后，随弹簧桅杆旋转缠绕收拢。[10]

The "Enlai 1" educational satellite adopts a hybrid storage design scheme, which is divided into three main parts: a deployment mechanism, a storage mechanism,

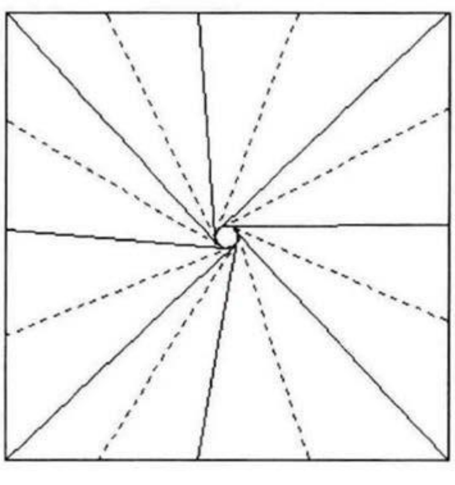

（b）环状褶折叠

and a locking mechanism. The ″ (″ type spring mast is used. After the brake sail film is folded, it is wound and folded with the rotation of the spring mast.[10]

图1.7 "恩来一号"教育卫星
″Enlai 1″ educational satellite

1.4 大型空间平台有控再入
Controlled reentry of large space platform

目前大型空间平台有控再入技术还处于设想前景阶段。
At present, the controlled reentry technology of large space platform is still in the stage of imagination.

增阻离轨有控再入是针对大型任务后航天器，大型航天器的一些部组件在重返大气到达地球表面后不能完全烧毁，可能危及地面人员和财产的安全， 因此需要有控、针对性的离轨和再入。[2]在充气式增阻离轨装置的有控再入过程中，当轨道降低至即将进入大气层时，增阻离轨装置排气，以减小气动阻力，推迟再入时间。之后利用精确的时间控制，在轨道上的特定位置再次充气。当满足预定的再入速度时，增阻离轨装置与卫星分离。该工作程序能使系统以可控的方式、有针对性的再入大气层，使大型航天器的残余碎片落入海洋，避免落在陆地。有针对性的再入能把地面人员伤亡和财产损失降低到可接受的水平。

Deorbit controlled reentry with augmented drag is aimed at large spacecraft after mission.Some components of large spacecraft can not be completely burned after re-entering the atmosphere and reaching the earth's surface, which may endanger the safety of people and property on the ground, so controlled and targeted deorbit and

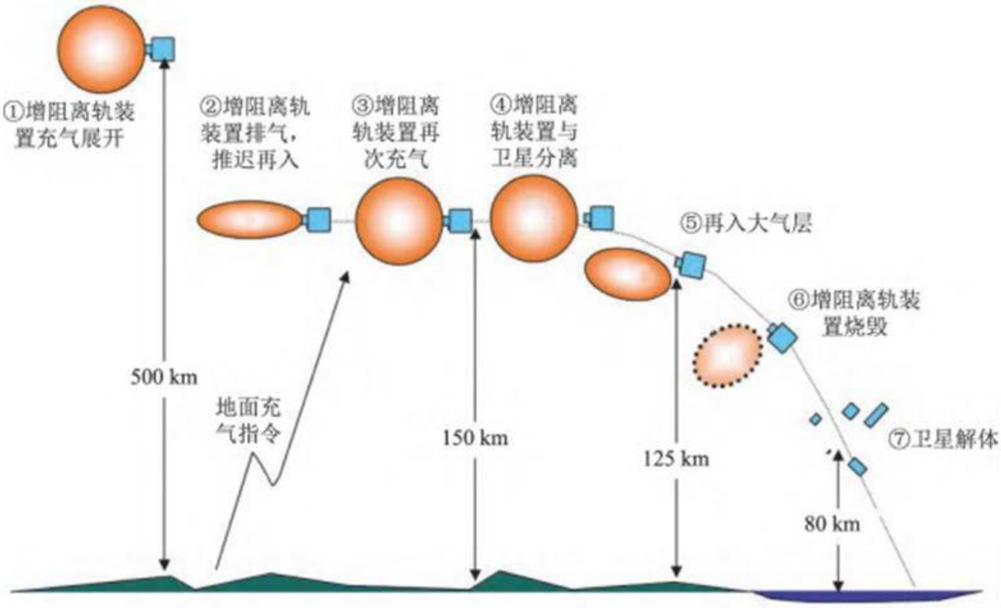

reentry are needed.[2]In the controlled reentry process of the inflatable drag augmentation deorbit device, when the orbit is lowered to the point where it is about to enter the atmosphere, the drag augmentation deorbit device exhausts to reduce aerodynamic drag and delay the reentry time. After that, with precise time control, it can be inflated again at a specific position on the track. When the predetermined reentry velocity is met, the drag augmentation deorbit device separates from the satellite. This working procedure enables the system to re-enter the atmosphere in a controlled and targeted manner, so that the residual debris of large spacecraft can fall into the ocean and avoid landing on land. Targeted reentry can reduce casualties and property damage on the ground to an acceptable level.

图1.8 有控再入的离轨操作概念
Concept of controlled reentry deorbit operation

1.5 本文主要内容
The main content of this paper

本文主要分为六个章节归纳所做工作： 第 1 章，

绪论。进行了背景调研。

This paper is divided into six chapters to summarize the work done: Chapter 1, Introduction. Background research was conducted.

第 2 章，任务分析。根据所调研的信息进行整合，提出本方案的具体任务目标，确定任务要求。

Chapter 2, Task Analysis. Integrate according to the investigated information, put forward the specific task objectives of this scheme, and determine the task requirements.

第 3 章，轨道设计。根据约束确定轨道设计。

Chapter 3, Track Design. The orbit design is determined based on the constraints.

第 4 章，有效载荷设计。介绍了有效载荷设计的具体过程和影响因素。

Chapter 4, Payload Design. The specific process and influencing factors of payload design are introduced.

第 5 章，分系统设计。阐述了对卫星的各个分系统的设计思路和结果，包括结构分系统、有效载荷、星载计算机等方面。

Chapter 5, Subsystem design. The design ideas and results of each subsystem of the satellite are described, including the structure subsystem, payload, on-board computer and so on.

第 6 章，总结。

Chapter 6, Summary.

2 任务分析 Mission analysis

2.1 任务描述 Task description

立方体卫星（CubeSat）研制周期短、成本低，可以用作为技术验证。本任务拟设计一个制动帆面积可控的立方星来进行在轨技术验证，该立方星的制动帆可以在预定轨道稳定展开，制动帆旋转改变迎风面积，并将姿态、位置等信息传回地面站。

CubeSat has a short development cycle and low cost, which can be used as a technical demonstration. In this task, it is planned to design a cubic satellite with controllable braking sail area for on-orbit technical verification. The braking sail of the cubic satellite can be stably deployed in a predetermined orbit. The braking sail rotates to change the windward area, and the attitude, position and other information are transmitted back to the ground station.

在功率、质量和体积有限的情况下，近地轨道上的小卫星主要通过重力梯度和气动阻力力矩来进行被动姿态稳定。本任务可利用制动帆提供的气动阻力进行立方星姿态稳定，可获取卫星传回的姿态信息，遂将验证制动帆作为姿态稳定装置的可行性作为次要任务目标。此外，若有效载荷失效，例如：制动帆未打开或面积不可控等故障，可将探测高层大气密度作为备用任务，卫星将姿态、位置、大气密度等信息传回即可。

In the case of limited power, mass and volume, small satellites in low earth orbit mainly use gravity gradient and aerodynamic drag torque to stabilize their attitudes passively. In this task, the aerodynamic resistance provided by the brake sail can be used to stabilize the attitude of the cubic satellite, and the attitude information sent back by the satellite can be obtained, so the feasibility of verifying the brake sail as an attitude stabilization device is taken as a secondary task objective. In addition, if the payload fails, for example, the brake sail is not opened or the area is uncontrollable, the upper atmospheric density can be detected as a backup task, and the satellite can send back information such as attitude, position and atmospheric density.

2.2 任务目标 Mission objectives

2.2.1 主要目标 The main goal

研究通过改变面质比实现控制卫星在 LEO 上的下落轨迹的可行性。

The feasibility of controlling the falling trajectory of a satellite on LEO by changing the area-to-mass ratio is studied.

2.2.2 从属目标

Slave target

（1） 验证制动帆作为被动姿态稳定装置的可行性。制动帆使卫星的压力中心在质量中心后面，提供气动力矩，保持卫星姿态。

To verify the feasibility of brake sail as a passive attitude stabilization device. The brake sail places the satellite's center of pressure behind the center of mass, providing aerodynamic torque to maintain the satellite's attitude.

（2） 探测高层大气密度，获取在卫星飞行过程中的不同位置的大气密度实测值。（在载荷失效时不受影响，作为备用任务）

Detect the density of the upper atmosphere and obtain the measured values of the atmospheric density at different positions during the flight of the satellite. (Not affected in case of load failure, as a backup task)

2.3 任务最高层系统要求
Mission Highest Level System Requirements

2.3.1 功能要求
Functional requirements

表2.1 功能要求
Table 2.1 Functional requirements

性能 Performance	在规定时间，制动帆稳定展开； At the specified time, the brake sail is unfolded stably; 按计划调节制动帆面积，改变迎风面积； 在任何迎风面积下保持俯仰和偏航姿态稳定； Adjust the brake sail area according to the plan and change the windward area; Maintain pitch and yaw attitude stability over any windward area;
覆盖率 Coverage	途径我国地面站 Through the ground station of our country
通信能力 Communication capability	在一定轨道周期内传回位置、姿态、加速度等信息 Return position, attitude, acceleration and other information within a certain orbital period
附属任务 Subordinate tasks	研究气动力矩对姿态的稳定效果 The effect of aerodynamic moment on attitude stability is studied.

2.3.2 运行要求
Operational requirements

表2.2 运行要求
Table 2.2 Operational requirements

总任务周期 Total mission period	300 天 300 days
存活能力 Ability to survive	考虑原子氧侵蚀、空间辐射环境 Atomic oxygen erosion and space radiation environment shall be considered
数据分配 Data distribution	将数据发送给我国的某一地面站 Send the data to a ground station in our country
数据内容 Data content	姿态、位置信息 Attitude and position information
轨道类型 Type of track	地球近地圆轨道 Earth's near-earth circular orbit

2.3.3 约束条件
Constraints

表2.3 约束条件
Table 2.3 Constraints

成本 Cost	预估 100 万（不包括试验、发射等） Estimated 1 million (excluding test, launch, etc.)
时间进度 Time	研制时间 1 年内 Development time within 1 year

schedule	
轨道约束 Orbital constraint	选择气动力主导的轨道高度，同时又为任务留出足够的余量（500- 650km），降交点地方时范围从8： Choosing an aerodynamically dominated orbital altitude while leaving sufficient margin for the mission (500-650 km), the range at the descending node is from 8: 00-16：00 的太阳同步轨道 Sun-synchronous orbit from 00 to 16:00
管理规定 Management regulations	符合国家法律政策要求 Meet the requirements of national laws and policies
政治因素 Political factors	符合相关法律法规规定 Comply with relevant laws and regulations
环境 Environment	空间微流星、辐射环境 Space micrometeor and radiation environment
发射约束 Launch constraint	作为从属载荷搭载发射 Launch as a slave payload

2.4 确定可选择的任务方案
Determine alternative task plan

可选择的任务方案如表 2.4 所示。
The alternative task schemes are shown in Table 2.4.

表2.4 可选择的任务方案
Table 2.4 Alternative Task Scheme

飞行任务的组成 Composition of the mission 单元 Unit	可选对象的内容 The contents of the optional object	最普通的可选对象 The most common optional object
有效载荷（制动帆及展开机构） Payload (brake sail and deployment mechanism)	构型 帆面材料驱动类型折叠方式支撑杆 Configuration sail surface material drive type folding mode support rod	方形、圆形、叶形、新型、螺旋桨型聚酰亚胺薄膜（Kapton）、聚脂薄膜 Square, round, leaf-shaped, new, propeller-type polyimide film (Kapton), polyester film （Mylar）等 (Mylar) et al. 外部电机驱动、弹性应变能 External motor drive, elastic strain energy Miura-Ori 折叠法、Frog-leg 折叠法、环状褶折叠法 充气桅杆、可卷曲桅杆 Miura-Ori fold, Frog-leg fold, annular pleat fold Inflatable mast, reelable mast
航天器平台 Spacecraft platform	推进系统姿轨控 电源 Attitude and orbit control power supply of propulsion system 结构 Structure	无 None 自旋、三轴；执行机构、敏感器太阳能帆板 Spin, triaxial; Actuator, sensor and solar panel 2U CubeSat
发射系统 Launch system	运载工具与发射场 Vehicle and launch site	无独立的发射任务，依赖其他航天任务的 Having no independent launch mission and relying on other space missions 发射 Launch
轨道 Track	高度 Height 倾角 星座 Dip Constellation	500-650km，低轨 500-650km, LEO 0°-180° 无 None
地面系统 Ground system	现有地面系统或专用系统 Existing ground system or dedicated system	
指令、控制和通 Command, control	及时性 Timeliness	存储和转储 Store and dump

and communication 信系统 Information System	控制和数据分发 Control and data distribution	单个或多个地面站 Single or multiple ground stations
飞行任务运行 Mission operations	自动化程度 Degree of automation	全自动地面站、24 小时全天运行 Fully automatic ground station, operating 24 hours a day

3 轨道设计
Track design

3.1 大气阻力约束
Atmospheric drag constraint

大气阻力是由于地球大气产生的对航天器运动的摄动力，阻力大小与大气密度、航天器形状和速度等因素有关。随着轨道高度的增加，大气密度急剧下降，因而气动力的影响力减弱。相应地，气动力对卫星的轨道和姿态影响能力也会减弱。

Atmospheric drag is a perturbation force produced by the earth's atmosphere on the motion of spacecraft, and the magnitude of drag is related to atmospheric density, spacecraft shape and speed. With the increase of orbit altitude, the atmospheric density decreases sharply, so the influence of aerodynamic force decreases. Accordingly, the influence of aerodynamics on the orbit and attitude of the satellite will be weakened.

表3.1 不同高度范围的主要环境力矩影响因素[13]
Table 3.1 Main environmental moment influence factors for different altitude ranges[13]

影响区 Zone of influence	轨道高度范围 Orbital altitude range	影响因素 Influencing factors
区域 1 Area 1	低于 300 km Less than 300 km	气动力矩占主导 Aerodynamic moment predominance
区域 2 Region 2	300 – 650 km	气动力矩与重力梯度力矩相当 The aerodynamic moment is comparable to the gravity gradient moment.
区域 3 Region 3	650 – 1000 km	气动力矩、重力梯度力矩和太阳 Aerodynamic Moments, Gravity Gradient Moments and the Sun 光压力矩相当 The photopressure moment is comparable
区域 4 Region 4	高于 1000 km Above 1000 km	太阳光压力矩和重力梯度力矩 Solar pressure moment and gravity gradient moment 占主导 Dominant

多数情况下，大气阻力被认为是对卫星工作不利的摄动力。但是对于利用大气阻力执行特定任务的卫星，必须为其选择合适的轨道高度。轨道高度的选择基于两种因素的权衡。由于气动姿态稳定依赖气动力矩大小，轨道高度要足够低。与此同时，为保证足够的在轨寿命，轨道高度不能过低，以避免轨道高度的快速损失。

In most cases, atmospheric drag is considered to be a perturbation force that is not conducive to the operation of satellites. However, for the satellite that uses atmospheric drag to perform specific tasks, it is necessary to select a suitable orbit altitude. The choice of orbital height is based on a trade-off between two factors. Because the aerodynamic attitude stability depends on the aerodynamic moment, the orbit altitude should be low enough. At the same time, in order to ensure sufficient on-orbit life, the orbit altitude should not be too low to avoid the rapid loss of orbit altitude.

作用于卫星的气动阻力：

Aerodynamic drag acting on satellite:

$$RR_{xx} = CC_{xx} \cdot \frac{\rho\rho \cdot vv^2}{2} \cdot SS \tag{3.1}$$

CC_{xx}为阻力系数。卫星全寿命周期内轨道高度处于 150km 至 500km 左右，处于自由分子流区域。在此区域内，气体分子的平均自由程远远大于卫星的尺寸，卫星所受的大气阻力几乎完全由独立的气体分子和卫星的相互作用决定。从卫星反射的分子和入射分子之间的碰撞产生的影响可以略去不计[4]。在这种情况下，

is the drag coefficient. In the whole life cycle of the satellite, the orbit altitude is about 150 km to 500 km, which is in the free molecular flow region. In this region, the mean free path of gas molecules is much larger than the size of the satellite, and the atmospheric drag on the satellite is almost entirely determined by the interaction between independent gas molecules and the satellite. The effects of collisions between the molecules reflected from the satellite and the incident molecules can be neglected[4]. In this case,

不同种类气体的阻力系数如下表所示。
The drag coefficients for different types of gases are shown in the table below.

表3.2 气体原子阻力系数[14]
Table 3.2 Gas atom drag coefficient[14]

气体种类 Type of gas	氢 Hydrogen	氦 Helium	氮 Nitrogen	氧 Oxygen	氩 Argon
阻力系数 C0 Drag coefficient C0	3.002	2.701	2.210	2.161	2.107

从大气模型[15]可知道，在 500 公里以下的自由分子流区域，大气主要成份
From the atmospheric model [15], it is known that in the free molecular flow region below 500 km, the atmosphere is mainly composed of

是氮、氧、氢、氦，而氮、氧占优势。在 500 公里以下的自由分子流区域，阻为系数可取$C_x = 2.2 \pm 0.2$。

It is nitrogen, oxygen, hydrogen and helium, and nitrogen and oxygen are dominant. In the free molecular flow region below 500 km, the drag coefficient is = 2.2 ± 0.2.

大气密度ρ的估算通常采用简化的大气模型[16]：
The atmospheric density is usually estimated using a simplified atmospheric model[16]:

$$\ln\rho = a - \bar{x}(h - h_0) \tag{3.2}$$

a，$\bar{x}$，h_0 为不同大气密度近似模型的常数，h为海拔高度。
? Is the constant of different atmospheric density approximation models, and is the altitude.

表3.3 大气密度估算模型
Table 3.3 Atmospheric density estimation model

模型 Model ABDC-59	高度 h Height H /km	Δρ /%
$a = -16.720$, $h_0 = 104000$, $\bar{x} = 0.01594$.	140	-14
	150	0
	200	4.5
	250	4
	300	-3
	400	2.5
	500	6.5
	700	5

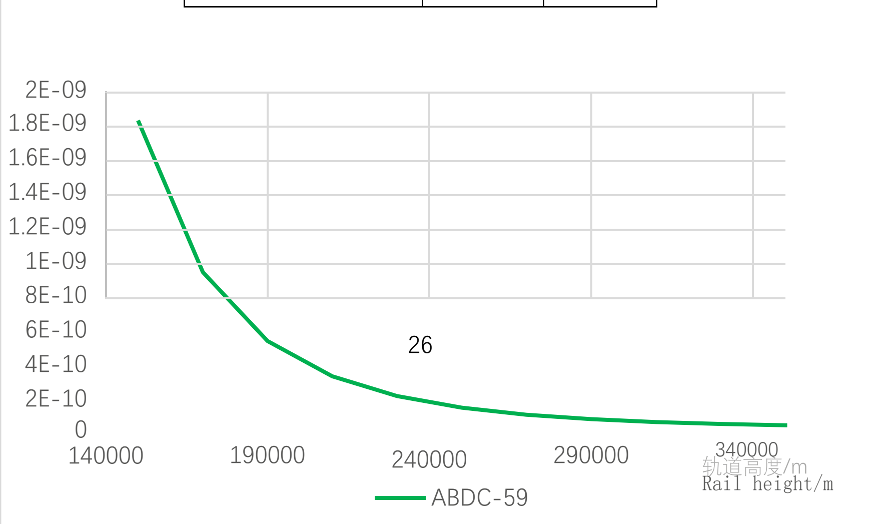

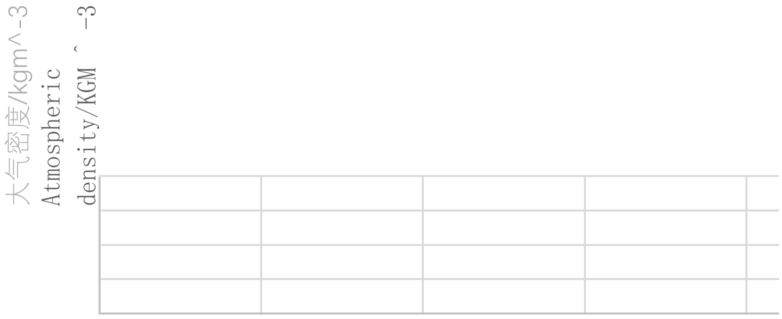

图3.1 大气密度
Atmospheric density

轨道寿命是人造卫星在轨道上存留的时间。它是从卫星进入轨道到陨落为止的时间间隔，近地卫星的轨道寿命取决于大气阻力。根据以上结果可计算轨道寿命。2U 大小的 CubeSat 最大许可重量为 2.6 千克，设定其迎风面积为 0.1 平方米和 0.44 平方米，即任务规定的最小和最大迎风面积。终止条件为轨道高度小于150km。分别计算了起始高度为 650km，632km，600km，550km，499km，450km对应的轨道寿命。

Orbital lifetime is the time that a satellite remains in orbit. It is the time interval from the satellite's entry into orbit to its fall. The orbital lifetime of a near-Earth satellite depends on atmospheric drag. Based on the above results, the orbital lifetime can be calculated. The 2 U-sized CubeSat has a maximum permissible weight of 2.6 kg and is set to have a frontal area of 0.1 m2 and 0.44 m2, the minimum and maximum frontal areas specified by the mission. The termination condition is that the orbit altitude is less than 150 km. The orbital lifetimes corresponding to the initial altitudes of 650 km, 632 km, 600 km, 550 km, 499 km and 450 km are calculated respectively.

其中，轨道高度 632km 和 499km 的太阳同步轨道为一些遥感卫星的常用轨道，可能有更多的搭载发射机会，因此被单独考虑。

Among them, the sun-synchronous orbit with orbit altitude of 632 km and 499 km is the common orbit of some remote sensing satellites, which may have more opportunities for piggyback launch, so it is considered separately.

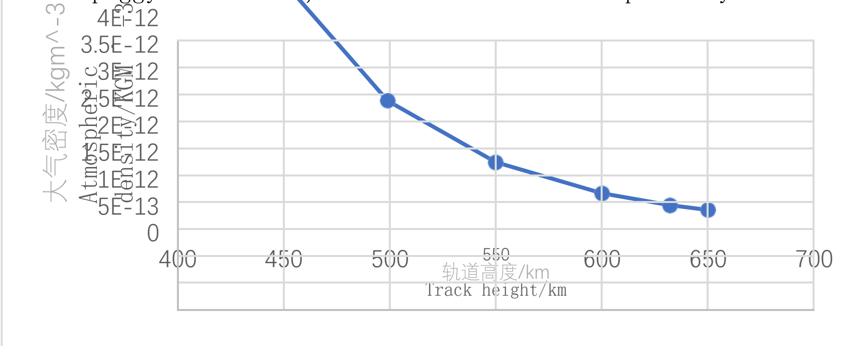

图3.2 轨道高度 450km~650km 范围大气密度变化

Atmospheric density variation at orbit altitude of 450km ~ 650km

在考虑的轨道高度范围内大气密度急剧变化，因此轨道寿命受高度影响非常显著。

The atmospheric density varies dramatically over the orbital altitude range considered, so the orbital lifetime is significantly affected by altitude.

为保证各项任务的顺利完成，卫星必须有足够长的最大轨道寿命，即卫星处于最小迎风面积时的轨道寿命。同时计算了最小轨道寿命，通过改变面质比，卫星的实际轨道寿命将介于二者之间。

In order to ensure the successful completion of various tasks, the satellite must have a long enough maximum orbit life, that is, the orbit life when the satellite is in the minimum windward area. At the same time, the minimum orbital lifetime is calculated, and the actual orbital lifetime of the satellite will be between the two by changing the area-to-mass ratio.

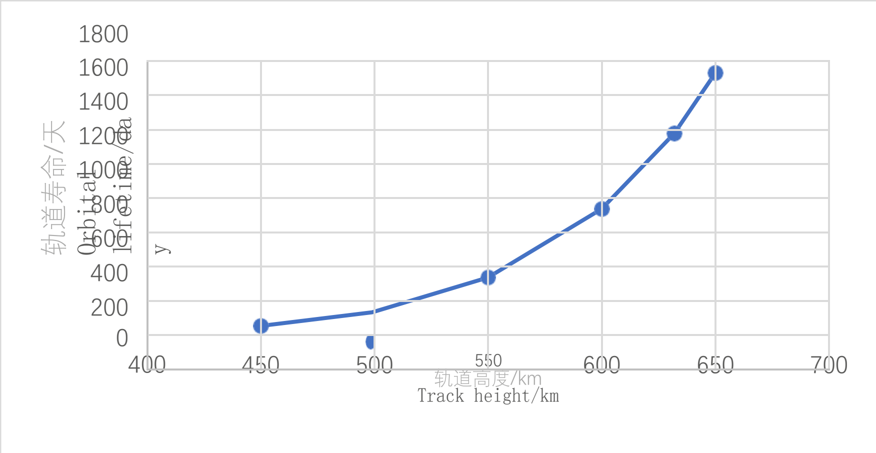

图3.3 最大轨道寿命

Maximum orbital lifetime

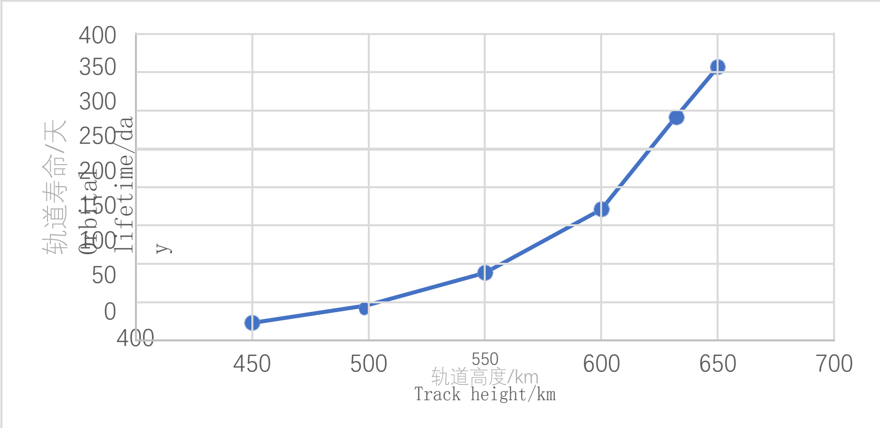

图3.4 最小轨道寿命

Minimum orbital lifetime

表3.4 大气阻力约束汇总

Table 3.4 Summary of atmospheric drag constraint

轨道高度 Orbital altitude /km	大气密度 Atmospheric density /kgm^-3	最大寿命 Maximum life /天 /day	最小寿命 Minimum life /天 /day
650	4.2E-13	1547.7	351.6
632	5.11E-13	1196.7	286.5
600	7.3E-13	756.5	166.5
550	1.3E-12	357.2	83.7
499	2.44E-12	155	41
450	4.64E-12	75	18.4

综上，可用的轨道高度范围为 550km 至 650km。在此高度下，大气阻力特性满足约束，同时可为任务保留了更大的灵活性。

To sum up, the available orbit altitude ranges from 550 km to 650 km. At this altitude, the atmospheric drag characteristics satisfy the constraints while preserving greater flexibility for the mission.

3.2 光照约束

Illumination constraint

CubeSat 采用体装式或展开式太阳能帆板，一般不具有自由度，因此必须考虑轨道的光照约束。一些元件，例如太阳敏感器的工作也需要保证规律的光照。因此对轨道类型的约束为太阳同步轨道（SSO）。

CubeSat uses body-mounted or deployable solar panels, which generally do not have degrees of freedom, so the illumination constraints of the orbit must be taken into account. Some components, such as sun sensors, also need to ensure regular illumination. The constraint on the orbit type is therefore a Sun-Synchronous Orbit (SSO).

晨昏线轨道能为太阳能帆板提供最为理想的光照条件，但是卫星在滚转方向上的姿态的不确定性会对太阳敏感器的安装造成困难。因此首先考虑降交点地方时在正午附近的太阳同步轨道。综合这些约束，降交点地方时的可用范围为9:00~15:00。

The twilight orbit can provide the most ideal illumination conditions for solar panels, but the uncertainty of the attitude of the satellite in the rolling direction will cause difficulties in the installation of solar sensors. Therefore, first co… node near noo… e of the desc…

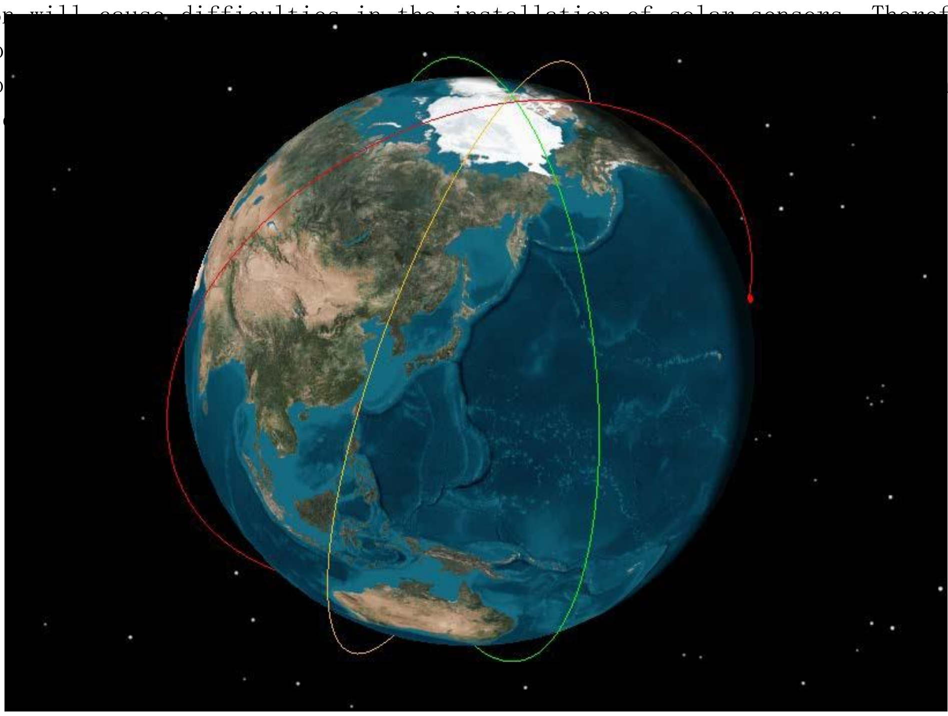

图3.5 符合条件的太阳同步轨道

Conditional Sun-synchronous Orbit

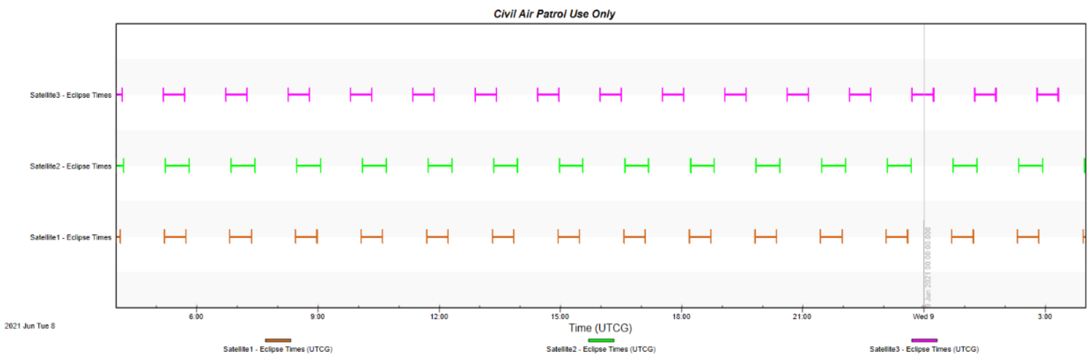

图3.6 不同降交点地方时地影区时长的微小差异

The slight difference of the duration of the local time shadow zone at different descending nodes

确定的轨道为降交点地方时 9:00，轨道高度 632km 的太阳同步轨道。

The orbit was determined to be a sun-synchronous orbit at an altitude of 632 km at 9:00 local time of the descending node.

3.3 轨道性能

Track performance

3.3.1 通讯条件

Communication conditions

由于卫星需要定期下传姿态信息和轨道高度以进行分析，需要考虑卫星可见性。为此计算了卫星到位于北京的地面站（39°59'N, 116°20'E）的可见性，统计周期为 210 天。设定仰角约束>30°。

Because the satellite needs to download the attitude information and orbit

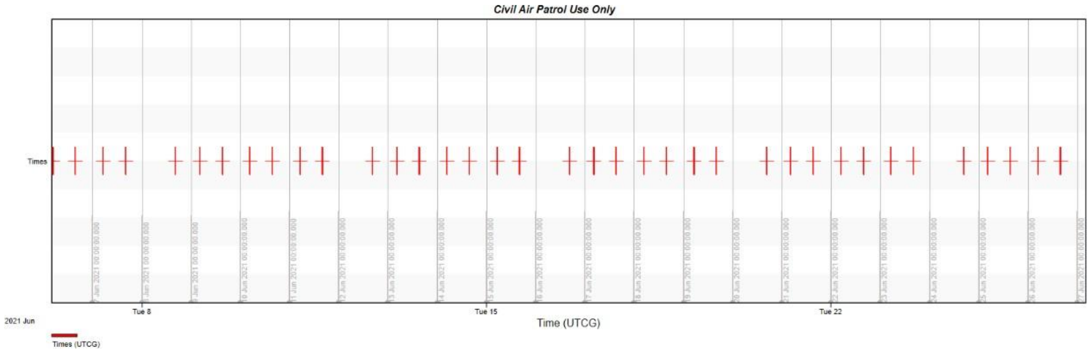

altitude periodically for analysis, the satellite visibility needs to be considered. For this purpose, the visibility of the satellite to the ground station (39 ° 59'N, 116 ° 20'E) located in Beijing was calculated with a statistical period of 210 days. Set the elevation constraint to > 30 ° .

图3.7 任务前21天可见性

Pre-Task 21 Days Visibility

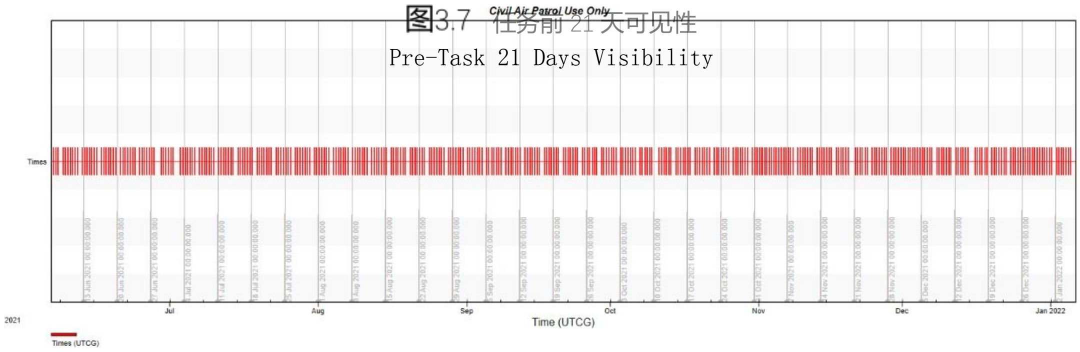

图3.8 全周期可见性表

3.5 可见性分析

Full Cycle Visibility

Table 3.5 Visibility analysis

可见性 Visibility	时间(s) Time (s)
最短可见 Shortest visible	32.511
最长可见 Longest visible	265.676

每24小时平均可见 Visible on average every 24 hours	210.954
总时间 Total time	78685.890

3.3.2 光照条件
Illumination conditions

分析卫星的光照时长和地影时长。在 STK 中建立场景，仿真时间段为
The illumination duration and the earth shadow duration of the satellite are analyzed. The scenario is established in STK, and the simulation time period is

2021 年6 月6 日04:00 至9 日04:00。
From 04:00 on June 6 to 04:00 on June 9, 2021.

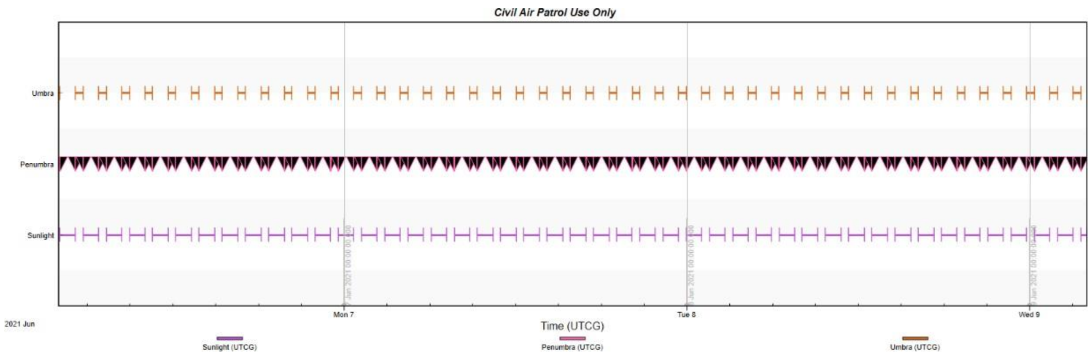

图3.9 光照分析
Illumination analysis

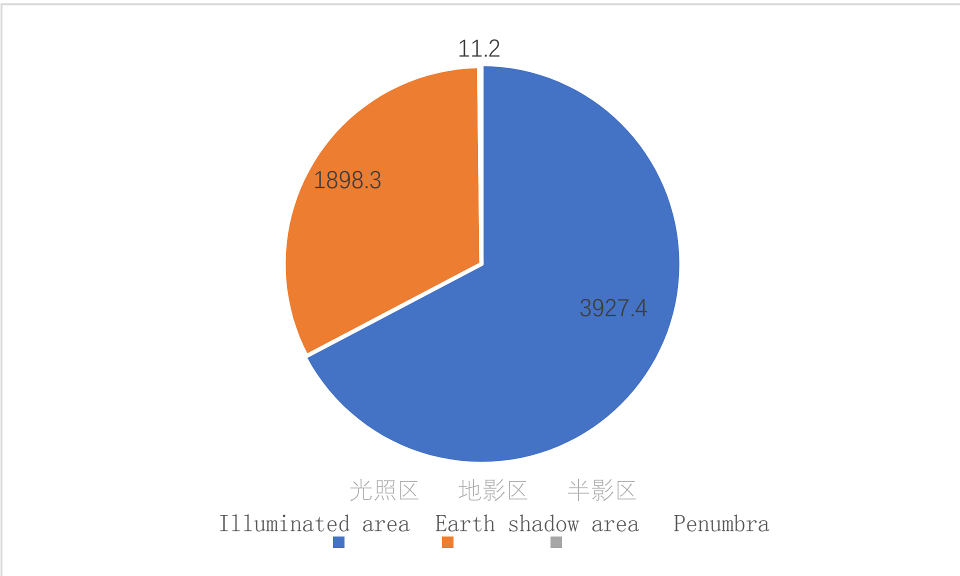

图3.10 一轨道周期内地影区时长，单位：s
Length of shadow area in an orbital period, unit: s

4 有效载荷
Payload

4.1 设计要求
Design requirements

本任务中，有效载荷为制动帆机构。任务目标要求制动帆具备以下功能特性：
In this task, the payload is the brake sail mechanism. The mission objective requires that the brake sails have the following functional characteristics:

（1） 能够按照需求调节迎风面积；
The windward area can be adjusted according to the requirement;

（2） 在任何展开状态下提供被动姿态稳定能力；
Provide passive attitude stabilization capability in any deployed state;

（3） 独立化、模块化，展开和运转过程对其他分系统没有不利影响；
Independence, modularization, and no adverse effect on other subsystems during deployment and operation;

（4） 高可靠性；
High reliability;

（5） 材料应具有较好的抗原子氧侵蚀能力；
The material shall have good atomic oxygen corrosion resistance;

（6） 无操作时自锁。
Self-locking when there is no operation.

与此同时，制动帆还需满足以下技术指标需求：
At the same time, the brake sail also needs to meet the following technical requirements:

（1） 最大迎风面积大于 0.4 平方米；
The maximum windward area is more than 0.4 square meters;

（2） 最小迎风面积小于 0.1 平方米；
The minimum windward area is less than 0.1 m2;

（3） 装置总体积小于 1U。
The total volume of the device is less than 1 U.

4.2 方案设计
Scheme design

4.2.1 制动帆基本方案
Basic scheme of brake sail

制动帆通过展开帆状薄膜，增大卫星的迎风面积，以增大卫星移动方向上的阻力。通常采用充气杆或弹性杆件作为骨架。目前已有的设计均提供巨大的迎风面积，用于快速降低轨道高度，还没有可控面质比，可作为执行机构的增阻机构。

The brake sail increases the windward area of the satellite by unfolding the sail-like membrane, so as to increase the resistance in the direction of satellite movement. Inflatable rods or elastic rods are usually used as the skeleton. The existing designs all provide a large frontal area for rapid reduction of the rail height, and there is no controllable area-to-mass ratio that can be used as a drag increasing mechanism for the actuator.

为完成控制下降轨迹的任务目标，本任务的制动帆需要按需求改变迎风面积，即改变卫星沿速度方向投影面积的大小。方法一般有改变增阻机构自身面积，和改变增阻机构投影面积大小。对于薄膜材料，展开后改变面积是不现实的，因此确定使用改变各面法向与速度的角度而改变迎风面积。

In order to achieve the mission goal of controlling the descent trajectory, the braking sail of this mission needs to change the windward area as required, that is, to change the size of the satellite's projected area along the speed direction. The methods generally include changing the area of the resistance-increasing mechanism itself and changing the projection area of the resistance-increasing mechanism. For the membrane material, it is not practical to change the area after deployment, so it is determined to change the windward area by changing the angle between the normal direction and the velocity of each surface.

4.2.2 结构
Structure

为保证制动帆在小迎风面积状态下均匀的气动外形，首先考虑了使用梯形的可活动制动帆帆板，此构型可在任何状态下保持气动姿态稳定，同时可采用成熟的展开机构和折叠方式。按照任务规定的迎风面积变化范围确定了帆板的外形尺寸。

In order to ensure the uniform aerodynamic shape of the brake sail in the state of small windward area, the trapezoidal movable brake sail is first considered, which can maintain the aerodynamic attitude stability in any state, and at the same time, the mature deployment mechanism and folding mode can be adopted. The overall dimensions of the sailboard are determined according to the change range of the windward area specified by the task.

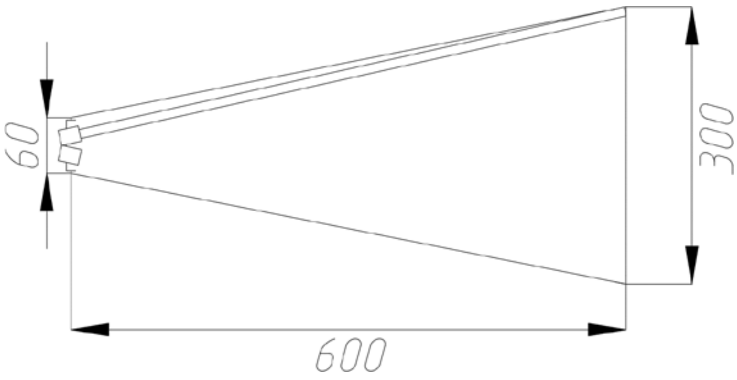

图4.1　单个帆板外形尺寸
Overall dimension of single sailboard

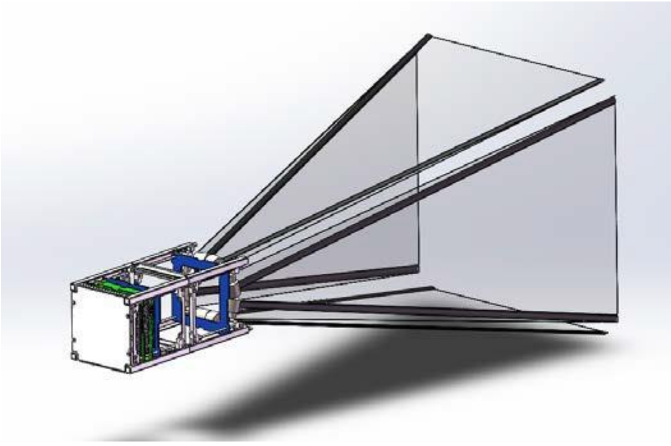

图4.2　最小迎风面积状态
Minimum frontal area state

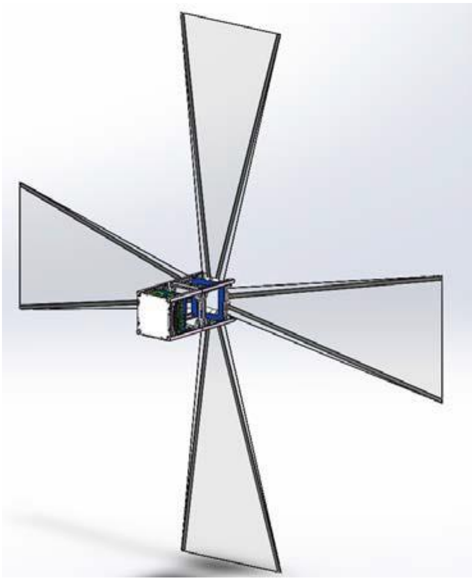

图4.3　最大迎风面积状态
Maximum windward area condition

进一步确定了结构。最大迎风面积 0.442m^2，最小迎风面积 0.09m^2。
The structure is further determined. The maximum windward area is 0.442$m^2$and the minimum windward area is 0.09m^2.

4.2.3 薄膜材料
Thin film material

制动帆材料的选择对增阻和阻力控制的有效性起着关键作用。目前市场上已有大量可购买的薄膜材料作为制动帆材料。很多高分子聚合物都已经运用于航天事业，其中多数都是聚酰亚胺材料，如 Kapton，这些薄膜材料的各种性能和参数都已经得到材料国际空间站实验室的验证，都有着良好的机械强度、尺寸稳定性、热回弹性和低释气特性[9]。

The choice of brake sail material plays a key role in the effectiveness of drag augmentation and drag control. At present, there are a large number of film materials available in the market as brake sail materials. Many polymers have been used in the aerospace industry, most of which are polyimide materials, such as Kapton. The properties and parameters of these film materials have been verified by the International Space Station Laboratory of Materials, and they all have good mechanical strength, dimensional stability, thermal resilience and low outgassing characteristics[9].

表4.1 薄膜材料性能参数[9]

Table 4.1 Performance parameters of film material[9]

材料 Material	极限温度 Limiting temperature /C°	原子氧侵蚀系数 Atomic Oxygen Erosion Coefficient $/10^{-24}cm^3/atom$	密度 Density $/g·cm^{-3}$	屈服强度 Yield strength /MPa
Kapton-HN Upilex-S CP-1 CORIN XLS Mylar	240 270 263 251 200	2.81 0.922 1.91 0.0305 4.01	1.42 1.47 1.54 1.54 1.39	231 549 87 79 196

在距地球表面 200~1000km 高度的 LEO 轨道空间中，存在着大量的原子氧。 这种原子氧会对各种高速飞行的航天器表面造成严重的侵蚀，造成表面材料的质量损失和性能下降[18]。在 MISSE 2 PEACE Polymers 任务中，进行了原子氧侵蚀实验。实验持续了 3.95 年，共测试了 40 种材料。

There is a large amount of atomic oxygen in LEO orbit at the altitude of 200 ~ 1000 km above the earth's surface. This atomic oxygen can cause severe erosion on the surface of various high-speed spacecraft, resulting in mass loss and performance degradation of surface materials[18]. Atomic oxygen erosion experiments were performed on the MISSE 2 PEACE Polymers mission. The experiment lasted 3.95 years and 40 materials were tested.

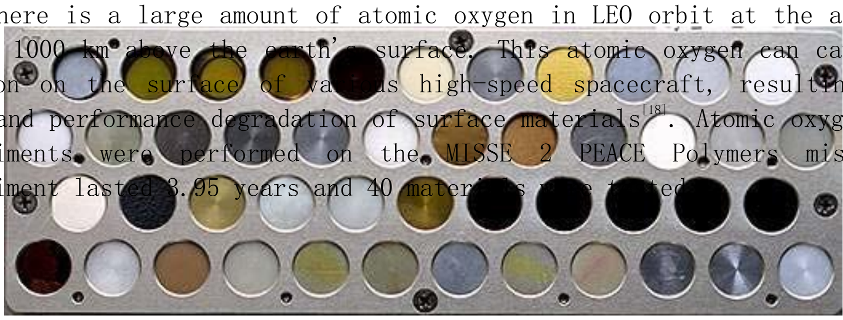

a. 实验前
Before the experiment

b. 实验后
After the experiment

图4.4 MISSE 2 PEACE Polymers 原子氧侵蚀实验[18]
MISSE 2 PEACE Polymers Atomic Oxygen Erosion Test[18]

可以发现，原子氧侵蚀会造成薄膜材料破损。对于本任务，制动帆长期工作，因此制动帆薄膜材料的设计与选型必须充分考虑侵蚀。制动帆薄膜在一段时间内的厚度损失由空间原子氧通量决定，而原子氧通量可通过大气和轨道参数来估算。暴露于原子氧冲击方向薄膜帆面的积累侵蚀深度可计算得

It can be found that atomic oxygen attack can cause damage to the thin film material. For this task, the brake sail works for a long time, so the design and selection of the brake sail membrane material must fully consider the erosion. The thickness loss of the brake sail film over time is determined by the space atomic oxygen flux, which can be estimated from atmospheric and orbital parameters. The accumulated erosion depth on the sail surface of the film exposed to the atomic oxygen impact can be calculated
[17]:

$$d = \int_{t0}^{t1} \rho_{AO}(h,t)v(h)\gamma_m dt \tag{4.1}$$

其中$\rho_{AO}(h, t)$是原子氧密度，是时间和轨道高度的函数。γ_m为原子氧侵蚀系数。$v(h)$是航天器和原子氧的相对速度。对于轨道高度恒定航天器，同 时忽略大气运动速度，这样侵蚀深度可按下计算：

Where $_O(,)$ is the atomic oxygen density as a function of time and orbital height. is the atomic oxygen erosion coefficient. () is the relative velocity of the spacecraft and the atomic oxygen. For a spacecraft with a constant orbital altitude and neglecting the atmospheric velocity, the erosion depth can be calculated as follows:

$$d = \rho_{AO}(h,t)v\gamma_m \Delta t \Delta \tag{4.2}$$

Δ为影响因子，是用于修正尾流和镀层对侵蚀的影响。对于单面镀层，且具有气动姿态稳定特性，Δ可取 0.05。

Is the influence factor, which is used to correct the influence of wake and coating on erosion. For a single-sided coating with aerodynamic attitude stabilization, 0.05 may be taken.

原子氧密度将随着轨道高度的降低而增加，为简化计算，采用离散法计算侵蚀深度。

The density of atomic oxygen will increase with the decrease of orbit height. In order to simplify the calculation, the discrete method is used to calculate the erosion depth.

表4.2 飞行天数和原子氧密度（MSISE90）

Table 4.2 Flight days and atomic oxygen density (MSISE90)

轨道高度范围 Orbital altitude range	最长飞行天数 Maximum flight days	ρ_{AO}/atom cm^{-3}
(600,632]	246.84	3.542E05
(500,600]	762.14	9.924E05
(400,500]	155.87	8.153E06
(300,400]	26.91	7.173E07

(200,300]	4.68	7.019E08
(150,200]	0.3	2.465E09

薄膜标准件为 15μm。全任务周期内对 Kapton 材料的侵蚀为 15.11 μm，需要使用镀层。Upilex-S 则为 4.95μm，无需额外的防护措施。同时考虑折叠和展开对强度的要求，相比使用镀层，15μm Upilex-S 更加符合要求。

The standard part of the film is 15 μm. The corrosion of Kapton material is 15.11 μm in the whole mission cycle, which requires the use of plating. Upilex-S is 4.95 μm and requires no additional safeguards. Considering the strength requirements of folding and unfolding at the same time, 15 μm Upilex-S is more in line with the requirements than using the coating.

4.2.4 折叠方式
Folding mode

使用三角形帆面的任务众多，因此三角形帆面的折叠方案也十分丰富和成熟。常用于薄膜折叠的方法有 Miura-Ori 折叠法和 Frog-leg 折叠法。

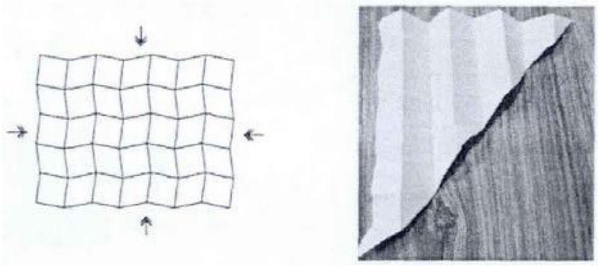

There are many tasks to use the triangular sail surface, so the folding scheme of the triangular sail surface is also very rich and mature. Commonly used methods for film folding are the Miura-Ori folding method and the Frog-leg folding method.

图4.5 Miura-Ori 折叠法
Miura-Ori folding method

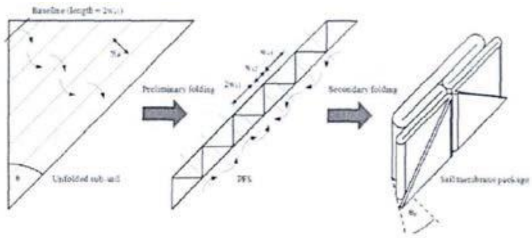

图4.6 Frog-leg 折叠法
Frog-leg folding method

本任务中使用到的帆面的特点是底角角度较大，因此需要测试实际折叠的性能。

The sail surface used in this task is characterized by a large base angle, so it is necessary to test the actual folding performance.

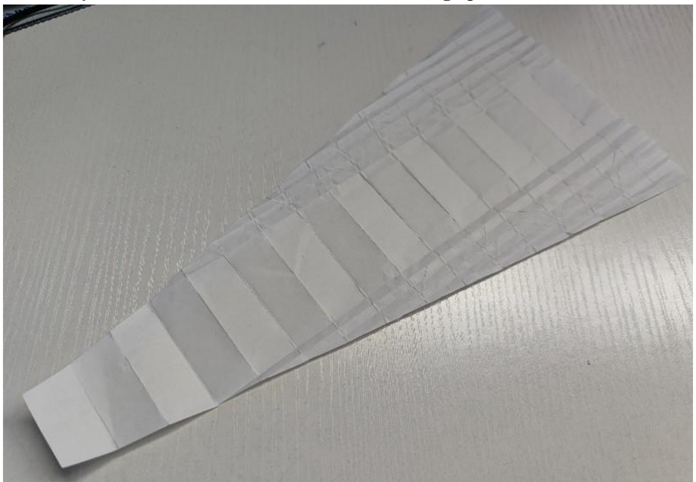

图4.7 帆布模型
Canvas model

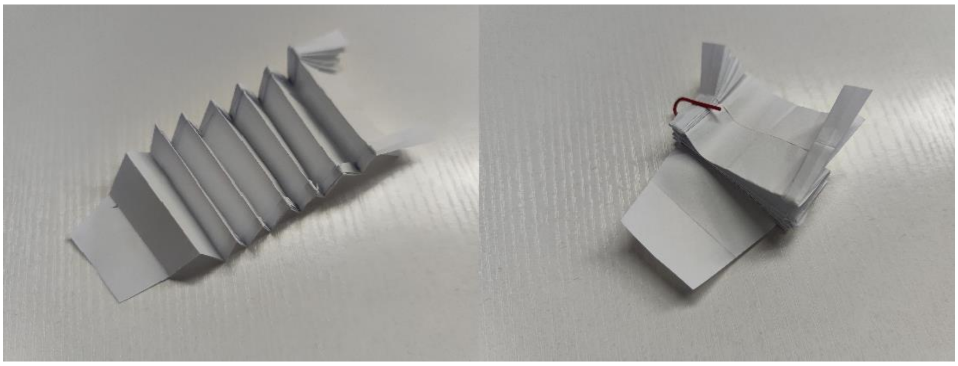

图4.8 折叠方法 1
Folding method 1

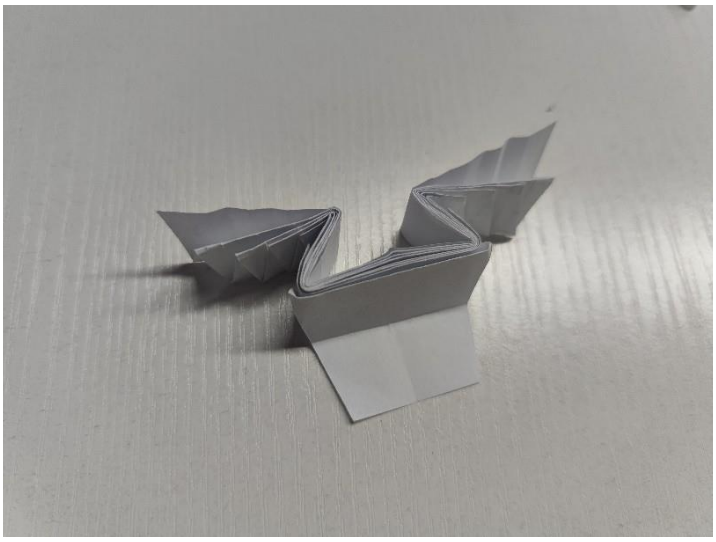

图4.9 折叠方法 2
Folding method 2

对比两种模式，得出折叠方法 2，即按照 Frog-leg 折叠法，可得到更好的展开性能。折叠后可压缩至 20mm×60mm 的尺寸轮廓内

By comparing the two modes, it is concluded that the second folding method, that is, the Frog-leg folding method, can get better unfolding performance. After folding, it can be compressed to the size outline of 20mm × 60mm.

图4.10 折叠方案
Folding scheme

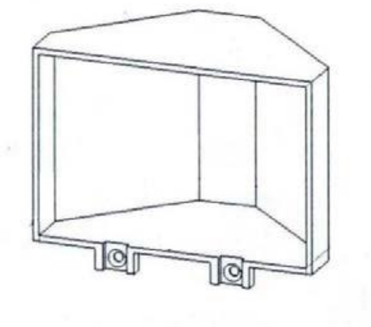

图4.11 帆的储存槽
Sail storage tank

4.2.5 弹性桅杆
Elastic mast

弹性桅杆用于展开帆面和保持帆面形状。这种弹性桅杆需要具有独特的力学性能，它可利用收拢时存储的弹性势能为制动帆的展开提供动力，也能够利用自身刚度为展开后的制动帆提供支撑，常常使用带状弹簧。

The elastic mast is used for spreading the sail surface and maintaining the shape of the sail surface. This kind of elastic mast needs to have unique mechanical properties. It can use the elastic potential energy stored when it is folded to provide power for the expansion of the brake sail. It can also use its own stiffness to provide support for the expansion of the brake sail, often using ribbon springs.

图4.12 不同材料的桅杆[19]
Mast of different material[19]

本任务中弹性桅杆具有超过 600mm 的伸展长度，适合用作天线。因此弹性桅杆必须采用合金材质。普通钢卷尺所使用的碳素钢，但是考虑碳素钢极易被磁化，从而产生磁偶极子，干扰卫星姿态和其他星载设备。因此弹性桅杆材料使用高弹性铜合金。

The flexible mast in this task has an extended length of more than 600 mm and is suitable for use as an antenna. Therefore, the flexible mast must be made of alloy. Ordinary steel tape uses carbon steel, but it is considered that carbon steel is easily magnetized, resulting in magnetic dipole, which interferes with satellite attitude and other on-board equipment. Therefore, the material of the elastic mast is a highly elastic copper alloy.

4.2.6 面质比控制

Surface to mass ratio control

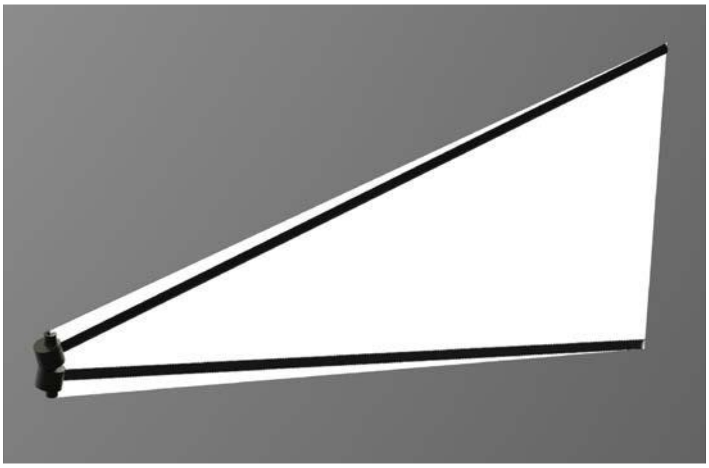

图4.13 帆板草图

Sailboard sketch

帆板通过绕安装轴转动改变与速度方向的夹角，这样在沿速度方向的投影面积改变，从而调节了面质比。每一个帆板通过一个齿轮传动机构，由驱动电机驱动。

The angle between the sailboard and the speed direction is changed by rotating the sailboard around the mounting shaft, so that the projection area along the speed direction is changed, and the area-mass ratio is adjusted. Each sailboard is driven by a driving motor through a gear transmission mechanism.

首先估算了帆板相对轴的最大力矩。作用于帆面的气动力大小R_x:

Firstly, the maximum torque of the sailboard relative to the axis is estimated. Aerodynamic force acting on sail surface :

$$R_x = C_x \frac{\rho \cdot v^2}{2} \cdot S \tag{4.3}$$

最大气动力出现在轨道高度最低的时刻，此时速度最大，空气密度也最大。按照公式 3.2 可计算大气密度。

The maximum atmospheric power occurs at the moment of the lowest orbital altitude, when the speed is the highest and the air density is the highest. The atmospheric density can be calculated according to Equation 3.2.

$$\rho\rho|_{150kkmm} = 1.794 \times 10^{-9}\ kkkk \cdot mm^{-3}$$

此时卫星速度：

Satellite speed at this time:

$$vv = \sqrt{\frac{\mu\mu}{rr + h}} = \sqrt{\frac{3.98 \times 10^{14}\ mm^{3} \cdot ss^{-2}}{(6371 + 150) \cdot 10^{3} mm}} = 7812.4 mm/ss \tag{4.4}$$

根据 3.1 节，CC_{xx}取 2.2。帆板的迎风面积为 0.108mm^2。可计算一个帆板受到的最大气动阻力：

According to Section 3.1, takes 2.2. The windward area of the sailboard is 0.108108^2. The maximum aerodynamic resistance of a sailboard can be calculated:

$$RR_{xx.mmmmxx} = CC_{xx} \cdot \frac{\rho\rho \cdot vv^2}{2} \cdot SS = 2.2 \times \frac{1.794 \times 10^{-9} \times (7812.4)^2}{2} \times 0.108 = 0.0130\ \mathrm{N}$$

帆板的气动中心距离转轴的坐标：

The coordinate of the distance between the aerodynamic center of the sailboard and the rotation axis:

$$xx_{cc.mmaa} = 0.3667 mm$$

对转轴的最大力矩：

Maximum torque to the shaft:

$$MM_{RR.mmmmxx} = RR_{xx.mmmmxx} \cdot xx_{cc.mmaa} = 0.004767\ NNmm$$

力矩非常小，因此对电机没有产生大扭矩的要求，可以使用普通直流电机。一般使用 3V 有刷直流电机，功率 2W 以下。

The torque is very small, so there is no requirement for the motor to produce a large torque, and a common DC motor can be used. Generally, a 3 V brushed DC motor with a power of less than 2 W is used.

传动机构采用蜗轮蜗杆机构以保证更精确的帆板角度控制，同时可保证不施加控制时自锁。

The transmission mechanism adopts a worm gear and worm mechanism to ensure more accurate control of the angle of the sailboard and can ensure self-locking when no control is applied.

5 分系统设计
Subsystem design

5.1 结构分系统
Structural subsystem

5.1.1 结构分系统概述
Structure Subsystem Overview

卫星结构分系统是支承卫星中有效载荷以及其他分系统的骨架，是连接并支撑各个分系统的仪器设备，使其形成完整的航天器整体，并具备规定的刚度和能承受运载火箭及地面运输时的各种力学环境。

The satellite structure subsystem is the framework supporting the payload and other subsystems in the satellite, connecting and supporting the instruments and equipment of each subsystem to form a complete spacecraft as a whole, and has the specified stiffness and can withstand various mechanical environments of the launch vehicle and ground transportation.

5.1.2 结构分系统设计依据
Design basis of structural subsystem

本组设计的立方星采用国际标准的结构形式，采用结构框架加横梁的组合方式，将立方星分割成多个 1U 组合的结构形式，便于形成货架产品供用户选择。外部包络具有标准结构型谱，便于相应的立方星部署器的标准化设计。

The cubic star designed in this group adopts the structural form of international standard, adopts the combination of structural frame and beam, and divides the cubic star into multiple 1U combinations, which is convenient to form shelf products for users to choose. The outer envelope has a standard structure type spectrum, which facilitates the standardized design of the corresponding CubeStar deployer.

5.1.3 结构分系统设计结果
Structural Subsystem Design Result

结构分系统外部结构标准如表所示。同时结构材料采用高强度硬铝合金，牌号为 7075-T651， 具有良好的比强度。内部尺寸通过定义标准CSKB(CubeSat Kit Bus)板，可以实现立方星内部组件的结构标准化。该板卡可安装于任意结构立方星，并且 CSKB 板设计为非对称结构，具有防插错功能，如图所示。

The external structure standards of the structure subsystem are shown in the table. At the same time, the structural material is made of high-strength hard aluminum alloy with the brand of 7075-T651, which has good specific strength. The internal dimensions allow for structural standardization of the CubeStar internal components by defining a standard CSKB (CubeSat Kit Bus) board. The board can be installed in any cubic star structure, and the CSKB board is designed as an asymmetric structure with anti-misinsertion function, as shown in the figure.

表5.1 标准立方星结构包络型谱

Table 5.1 Envelope spectrum of standard cubic star structures

立方星单元 Cubic star cell	横截面尺寸/mm Cross section size/mm （卫星出口横截面） (Cross section of satellite outlet)	长度尺寸/mm Length/mm （沿出口方向） (In the direction of the exit)
1U	100 ×100	113.5×1 =113.5
1.5U	100 ×100	113.5×1.5 =170.25
2U	100 ×100	113.5×2 =227.0
3U	100 ×100	113.5×3 =340.5

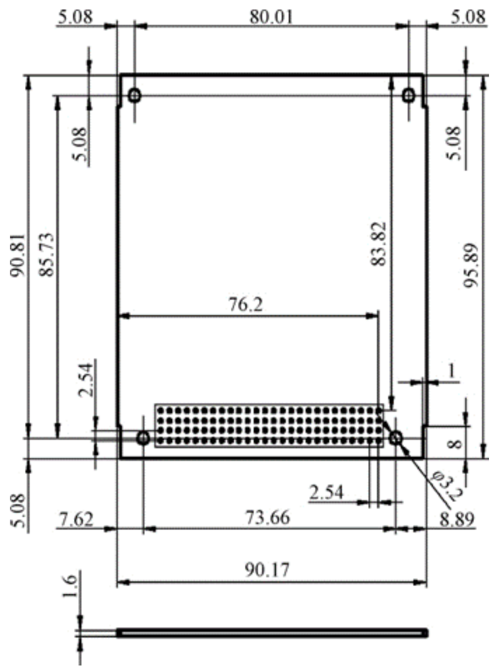

图5.1 立方星内部 CSKB 板接口标准

CubeStar Internal CSKB Board Interface Standard

根据计算，可使用展开式太阳能帆板解决帆板面积不足的问题，使得卫星的所有组件被安置在 2U 大小的空间内。因此卫星结构被确定为 2U CubeSat。卫星结构三维及二维示意图如图 5.2 和图 5.3 所示。选用 ISIS 2-UnitCubeSat，这是一种以立方体卫星为标准、通用的模块化卫星结构。外部贴太阳能电池片产生电能供应各分系统正常在轨工作。Cubesat 商店中给出了相应的模块。允许多个系统的安装配置，使开发人员在设计过程中具有最大的灵活性。具体参数和示意图如下，其中质量为 0.165kg，外体积为 100×100×227.0mm，内部其余系统可放置的体积为 98.4×98.4×196.8mm。卫星中各组件的坐标及质量分配如表 5.2 所示。

According to the calculation, the deployable solar panel can be used to solve the problem of insufficient area of the solar panel, so that all components of the satellite are arranged in a space of 2U size. The satellite structure is therefore determined to be 2U CubeSat. The three-dimensional and two-dimensional schematic diagrams of the satellite structure are shown in Figure 5.2 and Figure 5.3. ISIS 2-UnitCubeSat is selected, which is a modular satellite structure with CubeSat as the standard and common. And that electric energy generate by the externally pasted solar cell is supply to each subsystem for normal on-orbit operation. The corresponding modules are given in the Cubesat store. Allows installation configuration of multiple systems, giving developers maximum flexibility in the design process. The specific parameters and schematic diagram are as follows, in which the mass is 0.165 kg, the external volume is 100 × 100 × 227.0mm, and the volume of the rest of the internal system is 98.4 × 98.4 × 196.8mm. The coordinates and mass distribution of each component in the satellite are shown in Table 5.2.

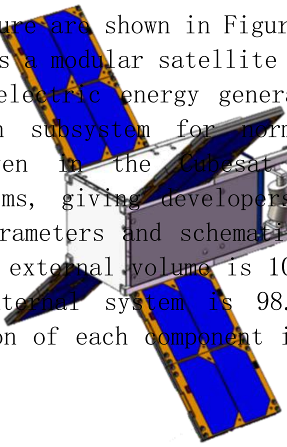

图5.2 卫星结构三维示意图

Three-dimensional schematic diagram of satellite structure

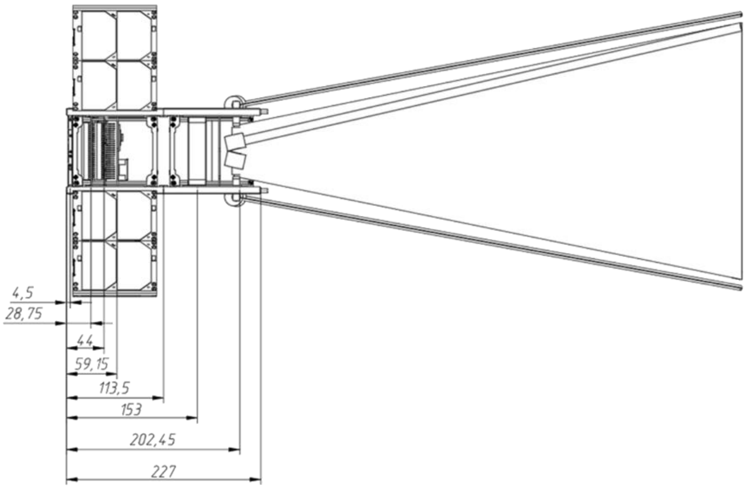

图5.3 卫星结构二维示意图
Two-dimensional schematic diagram of satellite structure

表5.2 各组件坐标及质量分配
Table 5.2 Coordinates and mass distribution of each component

组件 Component	坐标/mm Coordinates/mm	质量/g Mass/G
太阳敏感器 Sun Sensor	450	35
U/V 收发机 U/V transceiver	2875	75
计算机模组 Computer module	4400	94
传感器安装板 Sensor mounting plate	5915	100
电池片 Battery slice	5915	16×50
纵向结构件 Longitudinal structural member	11350	240
蓄电池 Battery	15300	310
制动帆机构 Brake sail mechanism	20245	300
	9984	1954

5.2 测控通信分系统
TT & C communication subsystem

5.2.1 测控通信分系统概述
Overview of TT & C communication subsystem

CubeSat 通信子系统作为 CubeSat 系统中最为重要的系统之一，承担着建立星地连接，实现可靠传输的责任。立方星星载通信系统多采用传统硬件结构收发信机，系统大多工作于 VHF/UHF 业余无线电频段。个别卫星如德克萨斯大学的 DTU-2 工作于 S 业余频段，大都

采用 AX.25 通信协议。

As one of the most important systems in CubeSat system, CubeSat communication subsystem is responsible for establishing satellite-ground connection and realizing reliable transmission. Cube-based satellite communication systems mostly use traditional hardware transceivers, and most of the systems work in the VHF/UHF amateur radio frequency band. Some satellites, such as the University of Texas' DTU-2, operate in the S amateur band and mostly use the AX.25 communication protocol.

在 VHF/UHF 频段，调制模式大多采用 AFSK 、BPSK 以及 GMSK 调制模式，在 S 或 X 频段多采用跳频方式，通信速率基本处于 0～100 kb/s 范围

In VHF/UHF band, AFSK, BPSK and GMSK modulation modes are mostly used, and frequency hopping mode is mostly used in S or X band, and the communication rate is basically in the range of 0 ~ 100 kb/s

内。在相同信噪比的情况下，BPSK 调制可以实现更低的误码率传输，更加适合于发射功率有限，对信道要求高的星地下行链路。而上行通信多采用AFSK 调制方式，适合于不受发射功率限制的地面站。由于考虑到我国的空间发射环境以及系统成本，在满足通信需求的前提下多采用 V/U 收发模式，即上行链路工作在 VHF 频段，下行链路工作在 UHF 频段。

Inside. Under the same SNR, BPSK modulation can achieve lower bit error rate transmission, which is more suitable for satellite downlink with limited transmission power and high channel requirements. Uplink communication mostly uses AFSK modulation, which is suitable for ground stations that are not limited by transmission power. Considering the space launch environment and system cost in China, the V/U transceiver mode is mostly used on the premise of meeting the communication needs, that is, the uplink works in the VHF band and the downlink works in the UHF band.

由于 CubeSat 本身体积限制，电池容量有限，卫星发射功率一般均小于

Due to CubeSat's size limitation and limited battery capacity, the satellite transmission power is generally less than

2W，如 ISIS 为 CubeSat 设计的 UHF/VHF 收发机发射功率仅达 0-2W。

2W. For example, the UHF/VHF transceiver designed by ISIS for CubeSat can only transmit 0-2 W.

通信分系统分为天线和收发器两部分，要求能够保障在有限的有效传输时间内完成信息的正常传递。

The communication subsystem is divided into two parts: antenna and transceiver, which is required to ensure the normal transmission of information within the limited effective transmission time.

关于天线部分，由于当前制动帆骨架以弹性金属片作为材料，且具有足够的长度，因此可将天线集成进制动帆模组，示意图如图 5.4 所示。天线设计为全向天线，展开长度 60.8 厘米。选用 ISIS Deployable antenna system for 1U/3U CubeSats，天线的示意图如图 5.5 所示，其参数如表 5.3 所示。

As for the antenna part, since the current brake sail framework is made of elastic metal sheet and has sufficient length, the antenna can be integrated into the brake sail module, as shown in Figure 5.4. The antenna is designed as an omnidirectional antenna with a deployed length of 60.8 cm. The ISIS Deployable antenna system for 1U/3U CubeSats is selected. The schematic diagram of the antenna is shown in Figure 5.5, and its parameters are shown in Table 5.3.

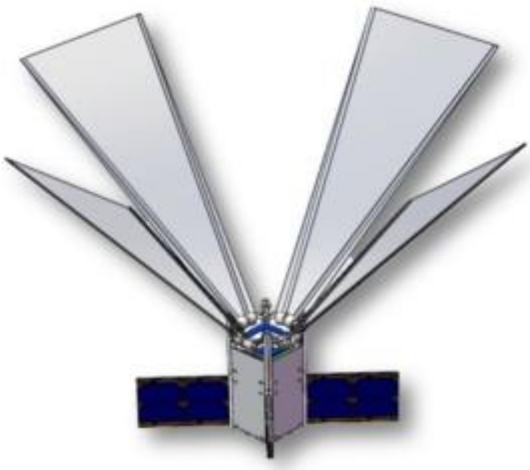

图5.4 天线集成进制动帆示意图
Schematic diagram of moving sail with integrated antenna

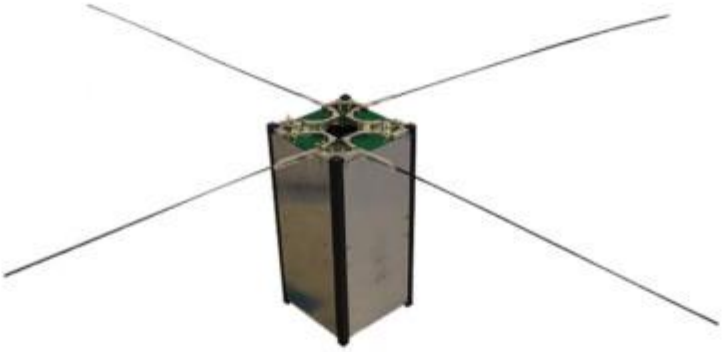

图5.5 ISIS Deployable antenna system for 1U/3U CubeSats 示意图
ISIS Deployable antenna system for 1U/3U CubeSats Schematic

表5.3 ISIS Deployable antenna system for 1U/3U CubeSats 参数表
Table 5.3 ISIS Deployable antenna system for 1U/3U CubeSats Parameter Table

项目 Project	性能参数 Performance parameters
频率范围 Frequency range	>10MHz
质量 Quality	<100g
电源电压 Supply voltage	3.3V/5V
功耗 Power consumption	40mW/60mW（部署期间 2W） 40mW/60mW (2 W during deployment)
工作温度 Operating temperature	-20℃~60℃
特点 Characteristic	全向天线，4 根 Omnidirectional antenna, 4
长度 Length	55cm
价格 Price	5500 欧元 5,500 euros

关于收发器部分，选用 ISIS UHF downlink/VHF uplink Full Duplex Transceiver。该收发器具有单板遥测、遥控和信标功能及全双工通信系统，且有低功耗、低质量、高度可配置等优点。高效的 BPSK 调制方案和灵活的下行超高频接收器可保证与CubeSat 进行通信。该模块采用 UHF 上行和 VHF 下行接收机，主要使用在低地球轨道上。采用了 400-470MHz 的上行传输和130-170MHz 的下行传输。TrxUV 数据传输速率从 1.2kbit/s 到 9.6kbit/ s 并可与 CubeSat 总线兼容，且可以与 ISIS 展开天线系统配合使用。该收发器的示意图如图 5.6 所示，其参数如表 5.4 所示。

For the transceiver section, the ISIS UHF downlink/VHF uplink Full Duplex Transceiver is selected. The transceiver has the functions of single-board telemetry, remote control, beacon and full-duplex communication system, and has the advantages of low power consumption, low quality and high configurability. An efficient BPSK modulation scheme and a flexible downlink UHF receiver guarantee communication with CubeSat. The module uses UHF uplink and VHF downlink receivers, and is mainly used in low earth orbit. Uplink transmission of 400-470MHz and downlink transmission of 130-170MHz are adopted. TrxUV data transfer rates range from 1.2 kbit/s to 9.6 kbit/s and are compatible with the CubeSat bus and can be used with the ISIS deployable antenna system. A schematic of this transceiver is shown in Figure 5.6, and its parameters are given in Table 5.4.

图5.6 ISIS UHF downlink/VHF uplink Full Duplex Transceiver 示意图
ISIS UHF downlink/VHF uplink Full Duplex Transceiver Schematic

表5.4 ISIS UHF downlink/VHF uplink Full Duplex Transceiver 参数表
Table 5.4 ISIS UHF downlink/VHF uplink Full Duplex Transceiver Parameter Table

项目 Project	性能参数 Performance parameters
质量 Quality	75g
尺寸 Size	90×96×15mm
电源电压 Supply voltage	6.5-20V
功耗 Power consumption	0.48W（接收）/4W（数据传输） 0.48 W (receive)/4 W (data transfer)
工作温度 Operating temperature	-20℃~60℃
发射机功率 Transmitter power	27dBm
发射机数据速率 Transmitter data rate	1200-9600bps
接收器数据速率 Receiver data rate	9600bps
接收机灵敏度 Receiver sensitivity	-104dBm BER
价格 Price	8500 欧元 8,500 euros

5.3 导航分系统
Navigation subsystem

5.3.1 导航分系统概述
Overview of navigation subsystem

该系统的目的是进行轨道和姿态的确定，保证航天器的稳定性。常用的姿态确定敏感

器有地球敏感器、太阳敏感器、星敏感器、陀螺仪、磁强计等。

The purpose of the system is to determine the orbit and attitude to ensure the stability of the spacecraft. Commonly used attitude determination sensors include earth sensors, sun sensors, star sensors, gyroscopes, magnetometers and so on.

5.3.2 选择依据

Selection basis

考虑到星敏感器虽然精度很高但是成本昂贵且需要两个星敏感器才能精

Considering that the star sensor has high precision, but the cost is expensive and two star sensors are needed to be accurate.

准定姿以及卫星的轨道为太阳同步轨道，为了取得尽可能准确的姿态信息，本卫星系统选择太阳敏感器、陀螺仪和磁强计作为姿态确定所使用的敏感器以及与星载计算机集成在一起的GPS 芯片模块作为轨道确认的敏感器。

In order to obtain the attitude information as accurate as possible, the satellite system selects a sun sensor, a gyroscope and a magnetometer as the sensors for attitude determination and a GPS chip module integrated with an on-board computer as the sensors for orbit confirmation.

5.3.3 敏感器设计结果

Sensor design results

1) SSOC D60 2-Axis 太阳敏感器
SSOC D60 2-Axis Sun Sensor

视角范围：∓60° 测量精度：0.3° 分辨率：0.05° 功耗：0.35W

Viewing angle range: 60 °
Measurement accuracy: 0.3 °
Resolution: 0.05 °
Power consumption: 0.35W
尺寸：60×30×12 mm
Size: 60 × 30 × 12 mm

重量：35g
Weight: 35 G

2) Honeywell HMR2300

尺寸：80x30.5x22.3 mm
Size: 80x30.5x22.3 mm

质量：28g 功率：0.45W

Mass: 28 G
Power: 0.45 W
工作温度：-40~85℃范围： 2 gauss,

Operating temperature: -40 ~ 85 ℃ Range: 2 Gauss,
分辨率：<70 μgauss
Resolution: < 70 μgauss

3) ANALOG ADIS16445 惯性传感器
ANALOG ADIS16445 Inertial Sensor

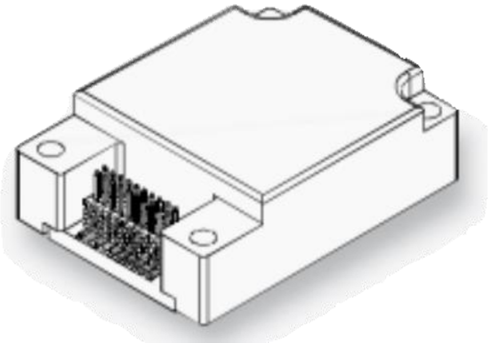

测量范围：∓250°/s启

动时间：175ms 功耗：

0.25W

Measurement range:
250 °/s Startup time:
175ms Power
consumption: 0.25W
尺寸：24.1x 37.7 x 10.8 mm
Dimensions: 24.1 X 37.7 X 10.8 mm

重量：15g
Weight: 15g

工作温度：-40~85℃
Working temperature: -40 ~ 85 ℃

在尽可能压缩成本以及保证敏感器精度满足需求的前提下，尽量选尺寸和重量小的敏感器。在对比多种敏感器元件的性能参数之后，最终决定使用上述所示的几种姿态敏感器。

On the premise of reducing the cost as much as possible and ensuring the accuracy of the sensor to meet the requirements, the sensor with small size and weight should be selected as far as possible. After comparing the performance parameters of various sensor elements, it was finally decided to use the attitude sensors shown above.

5.4 星载计算机分系统
On-board computer subsystem

5.4.1 星载计算机分系统概述
Summary of On-board Computer Subsystem

星载计算机(OBC)：也称星务计算机，负责星上数据与程序的存储、处理以及各分系统的协调管理，也称数管分系统，是计算机技术在空间环境下的应用,负责完成空间飞行器的控制和数据处理任务。恶劣的空间环境对星载计算系统的性能、可靠性和成本提出了巨大的挑战。在高昂的研究与制造费用、有限的硬件资源下，要确保海量数据处理的高可靠性是一项困难又关键的任务。

On-board computer (OBC), also known as housekeeping computer, is responsible for the storage and processing of on-board data and programs, as well as the coordination and management of various subsystems. It is also known as the data management subsystem. It is the application of computer technology in the space environment, and is responsible for completing the control and data processing tasks of spacecraft. The performance, reliability and cost of on-board computing systems are challenged by the harsh space environment. It is a difficult and critical task to ensure the high reliability of massive data processing under the high research and manufacturing costs and limited hardware resources.

5.4.2 星载计算机分系统功能要求
Functional Requirements for On-board Computer Subsystem

星载计算机的设计应配合整个飞行过程的任务要求来进行，在实现通过可变面质比的增阻帆实现 cubesat 星座的相位分布以及验证制动帆作为姿态稳定装置的可行性的任务中对星上计算机的要求有：

The on-board computer shall be designed in accordance with the mission requirements of the whole flight process. The requirements for the on-board computer in the mission of realizing the phase distribution of cubesat constellation through the drag increasing sail with variable area-mass ratio and verifying the feasibility of the brake sail as an attitude stabilization device are as follows:

1. 能够判断应该与地面站通信的时刻；
   Be able to judge the time of communication with the ground station;
2. 能够对确定增阻帆结构展开的时刻；
   The moment of deployment of the drag increasing sail structure can be determined;
3. 能够判断增阻帆面质比切换的时刻。

And can judge that switch time of the area-to-mass ratio of the drag increasing sail.

4. 具有足够的数据储存能力。
   Sufficient data storage capacity.

5. 具有足够的数据处理能力。
   Sufficient data processing capability.

5.4.3 星载计算机选择

On-board computer selection

1) 选择依据
   Selection basis

由于需要对地通信，定时将存储的信息发送给地面站。所以根据所选择的通信遥控遥测分系统的需要传输数据率和采样频率的大小确定星载计算机的部分指标。已知任务周期内 cubesat 卫星每次与北京地面站（仰角约束>30deg）的通信时间最低为为 32.511s，平均通信时间为 210.94s。通信遥控遥测分系统的发射机数据速率 1.2kbit/s 到 9.6kbit/ s，平均每次最可以传输248KB。星载计算机存储容量至少为，

The stored information is periodically transmitted to the ground station as required for communication. Therefore, according to the required transmission data rate and sampling frequency of the selected communication, remote control and telemetry subsystem, some indexes of the on-board computer are determined. It is known that the minimum communication time between cubesat satellite and Beijing ground station (elevation angle constraint > 30deg) is 32.511 s, and the average communication time is 210.94 s. The data rate of the transmitter of the communication, remote control and telemetry subsystem is 1.2kbit/s to 9.6kbit/s, which can transmit 248KB on average each time. The on-board compute has a storage capacity of at least,

2) 选择结果

Select the result

	ISIS-on-board-computer	Cube-Computer
处理器 Processor	400MHz 32 位ARM9 400MHz 32-bit ARM9	48MHz32 位ARM Cortex-M3 48 MHz 32-bit ARM Cortex-M3
闪存 Flash memory	256MB	4MB
SD 存储 SD storage	2×8GB	2GB
供电 Power supply	3.3V	3.3V
功率 Power	400mW	<200mW
尺寸 Size	96×90×12.4mm	90×96×10mm
质量 Quality	94g	50g~70g
工作温度 Operating temperature	-25~+65℃	-10~+70℃
单价 Unit Price	€4400	€4500

综合对比多款星上计算机，在存储空间、计算速率、尺寸、质量、供电电压、功率等关键参数上均可满足系统要求，但是 ISISPACE 400MHz ARM9 Module 成本更低。所以最后选取 ISISPACE 400MHz ARM9 Module 作为指令与数据处理分系统的星上计算机模块。

Compared with several on-board computers, the ISISPACE 400MHz ARM9 Module can meet the system requirements in terms of storage space, computing speed, size, quality, power supply voltage, power and other key parameters, but the cost is lower. Therefore, the ISISPACE 400MHz ARM9 Module is selected as the on-board computer module of the instruction and data processing subsystem.

3) 性能指标

Performance indicators

ISISPACE 400MHz ARM9 Module 的性能指标如下。

The performance specifications of the ISISPACE 400MHz ARM9 Module are as follows.

图5.7 ISISPACE 星上计算机模块表5.5

ISISPACE 星上计算机参数
ISISPACE On-Board Computer Module
Table 5.5 ISISPACE On-Board Computer Parameters

名称 Name	ISISPACE 400M Hz ARM9 Module
处理器 Processor	400MHz 32 位ARM9 400MHz 32-bit ARM9
闪存 Flash memory	256MB
SD 存储 SD storage	2×4GB
供电 Power supply	3.3V
功率 Power	400mW
尺寸 Size	96×90×12.4mm
质量 Quality	10g
工作温度 Operating temperature	-25~+65℃
单价 Unit Price	€4400

5.4.4 星载计算机分系统接口要求
On-board computer subsystem interface requirements

1) 电源接口
Power connector

电源接口是与电源分系统连接的电源供应接口，包括两个星务计算机和一个监控计算机的电源接口。三机的电源均为星上的二次电源。其中星务计算机的电源通过监控电路和监控计算机由继电器控制；监控计算机的电源直连在二次母线上，没有继电器控制。每个模块在电源入口处都分别进行了过流保护，以免电流过大烧毁电源。

The power interface is a power supply interface connected with the power subsystem, including the power interfaces of two satellite computers and a monitoring computer. The power supply of the three machines is the secondary power supply on the satellite. Wherein the power supply of the satellite computer is controlled by a relay through the monitoring circuit and the monitoring computer; The power supply of the monitoring computer is directly connected to the secondary busbar, and there is no relay control. Each module is separately over-current protected at the power supply inlet to prevent excessive current from burning the power supply.

2) 电信号接口

Electrical signal interface

电信号接口包括各种模拟、开关量的数据采集接口、星上总线接口、以及开关控制信号接口。与星载计算机相连的外部信号需要满足相关的电平要求和协议要求。电信号的机械接口统一采用 J-14 接插件。

The electrical signal interface includes various data acquisition interfaces for analog and switching values, on-board bus interface, and switch control signal interface. The external signals connected to the on-board computer need to meet the relevant level requirements and protocol requirements. The mechanical interface of the electrical signal adopts the J-14 connector.

3) 机械接口要求

Mechanical interface requirements

星载计算机电路板安装在卫星的层板上，安装孔位如图 1 所示。在连接处要好绝热处理。

The on-board computer circuit board is installed on the layer board of the satellite, and the mounting holes are shown in Figure 1. The joint shall be well insulated.

5.5 热控分系统

Thermal control subsystem

5.5.1 热控分系统概述

Overview of thermal control subsystem

按照自身是否具有根据需要自动调节温度的能力，卫星热控措施分为主动热控和被动热控两种。被动热控主要是依靠合理的卫星总体布局，按要求选取不同的热控硬件，正确组织卫星内外的热交换过程，使卫星的结构构件、仪器设备在高低温运行工况下都不超过允许的温度范围，以减小星内温度波动范围和冷热冲击，从而延长在轨卫星电子元器件和卫星的寿命。典型的被动热控方法有热控涂层、多层隔热材料、热管、相变材料、导热材料等。

According to whether it has the ability to automatically adjust the temperature according to its own needs, satellite thermal control measures can be divided into active thermal control and passive thermal control. Passive thermal control mainly relies on the reasonable overall layout of the satellite, selects different thermal control hardware according to the requirements, and correctly organizes the heat exchange process inside and outside the satellite, so that the structural components, instruments and equipment of the satellite do not exceed the allowable temperature range under high and low temperature operating conditions, so as to reduce the temperature fluctuation range and cold and heat shock in the satellite, thereby prolonging the life of electronic components and satellites in orbit. Typical passive thermal control methods include thermal control coatings, multilayer insulation materials, heat pipes, phase change materials, thermal conductive materials and so on.

5.5.2 热控分系统选择依据

Selection basis of thermal control subsystem

立方星具有高的热流密度和低的热惯性等持点，考虑太空中低重力、低温、空间外热流，卫星的尺寸和功率等因素。主动热控方式相较被动热控方式，温度控制效果更好。但是其成本远高于被动热控。而且由于 Cubesat 卫星并不需要进行严格的热量控制。出于成本控制的原因，本卫星拟采用被动热控方法解决 Cubesat 卫星的热控问题。由于技术方面的原因，微型热管加工难度和成本都很高，所以选择热控涂层、多层隔热材料作为热控分系统。

CubeSat has high heat flux and low thermal inertia, considering the factors of low gravity, low temperature, external heat flux, the size and power of the satellite. The temperature control effect of the active thermal control mode is better than that of the passive thermal control mode. But its cost is much higher than that of passive thermal control. And because the Cubesat satellite does not require strict thermal control. For the sake of cost control, the passive thermal control method is proposed to solve the thermal control problem of Cubesat satellite. Because of the technical reasons, the processing difficulty and cost of micro heat pipe are very high, so the thermal control coating and multi-layer thermal insulation material are selected as the thermal control subsystem.

5.5.3 热控分系统设计结果

Design results of thermal control subsystem

由于技术和成本的原因，本卫星系统采用的主要手段有：
For technical and cost reasons, the main means used in this satellite system are:

（1） 在主结构框架表面进行热控涂层处理，进而减少卫星内部热量的逸散。

Thermal control coating treatment is carried out on the surface of the main structure frame to reduce the heat dissipation inside the satellite.

（2） 使电池阵基板等温化（电池阵基板采用PCB-AL-PCB 夹层板， 在电池片间的空隙处贴镀金膜），减小太阳能电池因受热应力和热变形而被破坏的机率; 同时降低电池阵基板温度，提高太阳能电池的效率。

The battery array substrate is isothermalized (the battery array substrate adopts a PCB-AL-PCB sandwich board, and a gold-plated film is pasted at the gap between the cells), so that the probability that the solar cell is damaged due to thermal stress and thermal deformation is reduced; At that same time, the temperature of the array substrate is reduce, and the efficiency of the solar cell is improved.

（3） 出于对星内隔热、绝热的考虑，星内隔柱与结构间加隔热垫，电机与结构间加隔热垫，电池阵内部设置多层隔热组件。

In consideration of heat insulation in the satellite, a heat insulation pad is arranged between the partition column and the structure in the satellite, a heat insulation pad is arranged between the motor and the structure, and a multi-layer heat insulation component is arranged inside the battery array.

5.6 电源分系统

Power supply subsystem

5.6.1 电源分系统概述

Overview of power supply subsystem

卫星电源系统负责产生、储存、调节和分配电能，为有效载荷和其它服务和支持系统提供能源。常用技术手段为蓄电池和太阳能电池阵。电源系统是 Cubesat 卫星最容易发生故障的部分，在研制中应该充分强调可靠性。本卫星采用太阳能电池阵和 COTS 单体锂离子蓄电池。

Satellite power systems are responsible for generating, storing, regulating and distributing electrical energy to provide energy for payloads and other service and support systems. The common technical means are storage battery and solar cell array. The power supply system is the most vulnerable part of the Cubesat satellite, and the reliability should be fully emphasized in the development. The satellite uses solar cell array and COTS single lithium ion battery.

5.6.2 电源分系统选择依据

Selection basis of power supply subsystem

根据 Cubesat 卫星在一段时间内不同模式所消耗的总功率与太阳能电池阵产生的总功率能否达到平衡的条件来设计电源分系统。

The power subsystem is designed according to whether the total power consumed by different modes of Cubesat satellite in a period of time can reach a balance with the total power generated by the solar array.

(1) 划分工作模式

Divide the working mode

按照卫星工作情况的不同，将卫星划分为 4 种不同的模式，分别为部署模式（模式 1），工作模式（模式 2），通信模式（模式 3）和基本模式（模式

According to the different working conditions of the satellite, the satellite is divided into four different modes, namely deployment mode (mode 1), working mode (mode 2), communication mode (mode 3) and basic mode (model

4）。在部署模式下，卫星展开制动帆，之后根据需要在工作模式和非工作模式以及基本模式下进行切换。

4)。 In the deployment mode, the satellite deploys the brake sails, and then switches between the operational and non-operational modes and the basic mode as required.

(2) 不同工作模式的功耗

Power consumption in different operating modes

不同模式下各分系统消耗的功率如下表所示。这四种模式下的功耗分别为3.68W,9.68W，5.2W 和1.68W。

The power consumption by each subsystem in different modes is shown in the following table. The power consumption in these four modes is 3.68 W, 9.68 W, 5.2 W, and 1.68 W.

表5.6 工作模式

Table 5.6 Working mode

类别 Category		部署模式 Deployment mode	电机工作模式 Motor operating mode	通信模式 Communication mode	基本模式 Basic mode
执行机构 Actuator	制动帆驱动电机 Brake sail drive motor	0W	8W	0W	0W
	制动帆展开机构 Brake sail deployment mechanism	2W	0W	0W	0W
姿态敏感单元 Attitude sensing unit	三轴磁强计 Triaxial magnetometer	0.2W	0.2W	0.2W	0.2W
	陀螺仪 Gyroscope	0.25W	0.25W	0.25W	0.25W
	太阳敏感器 Sun Sensor	0.35W	0.35W	0.35W	0.35W
通讯系统 Communication system	U/V 收发机 U/V transceiver	0.48W	0.48W	4W	0.48W
指令处理单元 Instruction Processing Unit	星载计算机模块 On-board computer module	0.4W	0.4W	0.4W	0.4W
总计 Total		3.68W	9.68W	5.2W	1.68W

1. 由于部署模式用时较短，在计算时可以暂时忽略。
   Because the deployment mode takes a short time, it can be temporarily ignored in the calculation.

2. 若采用基本模式工作：光照区为基本模式，功耗为 1.68W；阴影区为基本模式，功耗为 1.68W；

   If the basic mode is used, the power consumption is 1.68 W when the illumination area is in the basic mode; The shaded area is the basic mode and the power consumption is 1.68 W;

3. 若采用通信模式：光照区为非工作模式，功耗为 5.2W；阴影区为基本模式，功耗为 1.68W；

   If the communication mode is used, the illumination area is in the non-working mode, and the power consumption is 5.2 W; The shaded area is the basic mode and the power consumption is 1.68 W;

4. 若采用电机工作模式：光照区为工作模式，功耗为 9.68W；阴影区为基本模式，功耗为 1.68W。

   If the motor working mode is adopted, the power consumption is 9.68 W in the working mode of the illumination area; The shaded area is the basic mode, which consumes 1.68 W.

5.6.3 电源分系统设计结果

Design results of power supply subsystem

1) 太阳能电池阵
Solar Array

太阳能电池片的种类不多，性能基本一致。所以在考虑成本的条件下，选择了下面这款太阳能电池片。

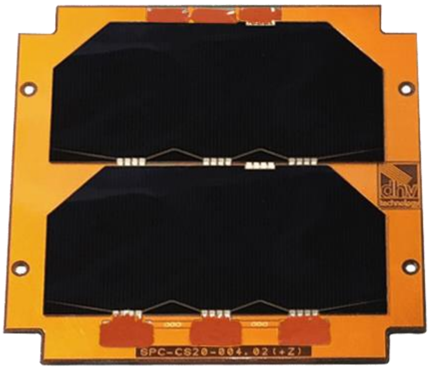

There are not many kinds of solar cells, and their performance is basically the same. Therefore, under the condition of considering the cost, I chose the following solar cell.

图5.8　太阳能电池片
Solar cell

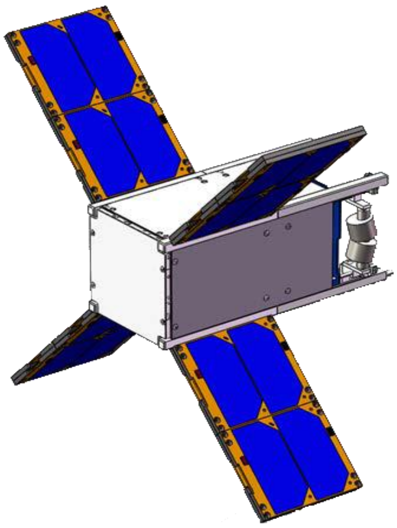

图5.9　展开式太阳翼
Deployable solar wing

太阳能电池片的具体技术指标如下表所示：
The specific technical indicators of solar cells are shown in the following table:

表5.7　　太阳能电池片性能参数

Table 5.7 Performance parameters of solar cell

配置 Configurati on	AM0 WRC = 1367 W / m2； T = 28° C； 串联配置 Series configuration
开路电压（Voc ） Open circuit voltage (Voc)	5.4V
短路电流（ISC） Short-circuit current (ISC)	0.52A
最大功率时电压（Vmp） Voltage at maximum power (Vmp)	4.82V
最大功率时电流（Imp） Current at maximum power (Imp)	0.5A
效率 Efficiency	30%
标称厚度 Nominal thickness	1.6mm±10%
工作温度 Operating temperature	-120℃~150℃
质量 Quality	50g
尺寸 Size	82.5mmx 98mmx 2.4mm

2) 锂离子蓄电池

Lithium ion battery

蓄电池组是卫星的供电储能装置，向卫星用电器提供电能以及储存太阳能电池阵产生的电能。

The storage battery is the power supply and energy storage device of the satellite, which provides electric energy for the electrical appliances of the satellite and stores the electric energy generated by the solar array.

COTS 单体锂电池不仅其容量满足上述容量要求，而且技术和工艺成熟，能量密度大，成本低廉，生产周期短，扩展性强，而且寿命和温度特性比传统电池都有大幅提升，对于减轻电源系统重量、提高能源利用效率和降低成本均有重要作用。

COTS single lithium battery not only meets the above capacity requirements, but also has mature technology and process, high energy density, low cost, short production cycle, strong expansibility, and its life and temperature characteristics are greatly improved compared with traditional batteries, which plays an important role in reducing the weight of power supply system, improving energy efficiency and reducing costs.

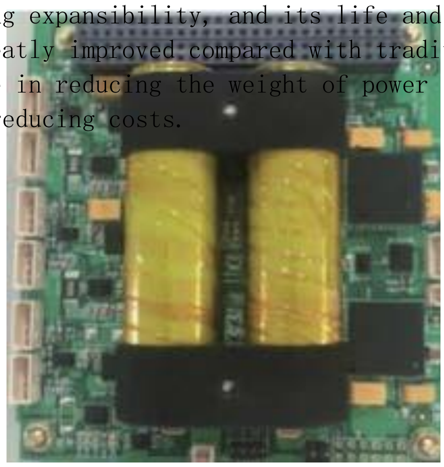

图5.10 蓄电池模块
Battery module

COTS 单体锂电池的技术指标如下表所示：
The technical indicators of COTS single lithium battery are shown in the following table:

表5.8　　蓄电池主要参数

Table 5.8 Main parameters of battery

名称 Name	COTS 单体锂电池 COTS single lithium battery
容量 Capacity	2.6Ah
额定电压 Rated voltage	3.7V
功率总容量 Total power capacity	9.62Wh
尺寸 Size	82.5mmx 98mmx 2.4mm

5.7　校核
Check

5.7.1 重量校核
Weight check

表5.9　　重量校核

Table 5.9 Weight check

组件 Component	坐标/mm Coordinates/mm	质量/g Mass/G
太阳敏感器 Sun Sensor	4.50	35
U/V 收发机 U/V transceiver	28.75	75
计算机模组 Computer module	44.00	94
传感器安装板 Sensor mounting plate	59.15	100
电池片 Battery slice	59.15	16×50
纵向结构件 Longitudinal structural member	113.50	240
蓄电池 Battery	153.00	310
制动帆机构 Brake sail mechanism	202.45	300
总计 Total	99.84	1954

Cubesat 卫星的每一 U 的质量上限为 1.3kg。由于本卫星的体积大小为2U，所以其质量上限为 2.6kg。经过汇总计算，得到卫星整星质量为 1954g。由于整形质量不超过 2kg，低于质量上限，所以卫星质量满足要求。

The Cubesat satellite has an upper mass limit of 1.3 kg per U. Since the size of this satellite is 2 U, the upper limit of its mass is 2.6 kg. After summary calculation, the mass of the whole satellite is 1954 G. Since the shaping mass is not more than 2 kg, which is lower than the upper mass limit, the satellite mass meets the requirements.

5.7.2 功耗校核

Power consumption check

(1) 光照条件

Illumination conditions

取 2021 年 6 月 6 日 04:00 至 9 日 04:00 作为数据时间段进行仿真，一个

From 04:00 on June 6, 2021 to 04:00 on June 9, 2021 is taken as the data time period for simulation.

轨道周期内光照时间T_d为 3927.4 秒，地影时间T_e为 1893.3 秒。

The illumination time T_d in the orbital period is 3927.4 seconds, and the earth shadow time T_e is 1893.3 seconds.

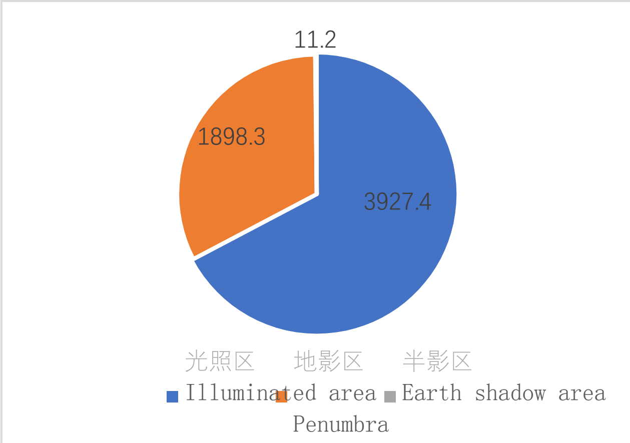

图5.11 一轨道周期内地影区时长，单位：s

Length of shadow area in an orbital period, unit: s

(2) 太阳电池阵需要产生的功率输出

Power output required to be generated by the solar array

全任务周期内，到北京的地面站（仰角约束>30deg），平均每 24 小时可见 367.69s，通信模式的时长为 24.78S，基本模式工作时长为 3902.62S。

In the whole mission cycle, the ground station in Beijing (elevation angle constraint > 30deg) is visible for 367.69 seconds every 24 hours on average, the duration of communication mode is 24.78 seconds, and the duration of basic mode is 3902.62 seconds.

一个周期内在不考虑电机工作模式的情况下，太阳电池阵需要产生的能量输出

The energy output required to be generated by the solar array in a cycle, regardless of the operating mode of the motor

$$W_{sa} = \left(\frac{P_e T_e}{X_{ed}} + \sum \frac{P_d T_d}{X}\right)$$

$P_e = 1.68W$ 星上设备地影区平均功耗

P_e 1.68 W average power consumption of on-board equipment in the shadow area

P_d星上设备光照区平均功耗，视 Cubesat 工作模式而定；

The average power consumption of $P_d$on-board equipment in the illumination area depends on the Cubesat working mode;

T_e地影区时间；T_d

光照区时间；

$T_e$time of earth shadow area;

$T_d$time of illumination area;

X_e太阳电池阵经蓄电池组到载荷的输出效率；X_d太阳电

池阵到载荷的输出效率。

Output efficiency of $X_e$solar array to load via battery pack; Output efficiency of $X_d$solar array to load.

$X_e = 0.7$； X_d

$= 0.85$。

则：
Then:

$$W_{sa} = \frac{P_e T_e}{X} + \sum_{ed} \frac{P_d T_d}{X} = \left(\frac{1.68 \times 1898.3}{0.7} + \frac{1.68 \times 3902.62}{0.85} + \frac{5.2 \times 24.78}{0.85}\right) = 12.421\text{KJ}$$

(3) 卫星寿命初期，太阳能电池片单位面积产生的功率
Power generated per unit area by solar cells at the beginning of the satellite's life

$$P_{BOL} = S \times \eta_{SC} \times AVE\left\{\sum_{n=1}^{4} \cos\theta_n\right\} \times I_d$$

其中，S:太阳照度常数 1367W/m²;
Where, S: solar illumination constant 1367W/m²;

η_{SC} 太阳电池片 i 的效率；取 0.3。
SC efficiency of solar cell I; Take 0.3.

$AVE\left\{\sum_{n=1}^{4}\cos\theta_n\right\}$ 根据经验取为 0.92
As a rule of thumb, 0.92

Id：过滤因子，取 0.75。可得

P_{BOL}=283.24W/m²。

Id: Filter factor, take 0.75. PBOL = 283.24 W/m² is obtained.

(4) 计算卫星寿命末期，太阳电池阵功率输出
Calculate the solar array power output at the end of satellite life

$$P_{EOL} = P_{BOL} \times L_d$$

其中，太阳电池片降级因子
Wherein the degradation factor of the solar cell

$L_d = \eta_{uv} \times \eta_{tc} \times \eta_m \times \eta_r \times \eta_{con} \times \eta_s \times \eta_{rad} \times \eta_t \times \eta_{op}$ η_{uv}：紫外线引起的功率损失(0.98)；

$L_d = \eta_{uv} \times \eta_{tc} \times \eta_m \times \eta_r \times \eta_{con} \times \eta_s \times \eta_{rad} \times \eta_t \times \eta_{op}$ η_{uv}: power loss due to ultraviolet light (0.98);

η_{tc}：热循环引起的功率损失 (0.99);
η_{tc}: power loss due to thermal cycling (0.99);

η_m：电池片不匹配引起的功率损失 (0.975);
η_m: power loss caused by cell mismatch (0.975);

η_r：电池片内阻引起的功率损失 (0.98)； η_{con}：外部污染源引起的功率损失(0.99)； η_s：外部遮挡引起的功率损失 (1)；

$_r$: Power loss caused by internal resistance of cell (0.98); η_{con}: power loss caused by external pollution source (0.99); η_s: power loss due to external occlusion (1);

η_{rad}：辐射损伤引起的功率损失η_t： 取 0.88;

η_{rad}: power loss caused by radiation damage η_t: 0.88;

η_{op}：在轨道位置太阳照度常数调节(1)。

η_{op}: solar illumination constant adjustment at orbital position (1).

所以：

So $$P_{EOL} = P_{BOL} \times L_d = 222.46\text{W/m}^2$$

(5) 计算在卫星寿命末期，太阳电池阵输出的功率

Calculate the output power of the solar array at the end of the satellite's life

$$A_{SA} = 4 \times 0.098 \times 0.0825 = 0.03234\,\text{m}^2$$

$$P = A_{SA} \times P_{EOL} = 7.194\text{W}$$

(6) 评估实际的太阳电池阵是否满足要求

Evaluate whether the actual solar array meets the requirements

$$W = P \times T_d = 7.194 \times 3927.4 = 28.254KJ > 12.421\mathrm{KJ} = \mathrm{W_{SA}}$$

则其能满足基本需求。

It can meet the basic needs.

太阳电池阵产生的多余的能量可以用来驱动电机，调节面质比。则电机

The excess energy generated by the solar array can be used to drive the motor and adjust the area-to-mass ratio. Then the motor

工作的时间 $t = \frac{(\mathrm{W} - \mathrm{W_{SA}}) \times 0.8}{} = 1583.3\mathrm{S}$。

Working time t = W - WSA 0.8 8 = 1583.3S.

则卫星在电机工作模式下可以工作 1583.3S。

The satellite can work at 1583.3S in the motor working mode.

6 总结
Sum up

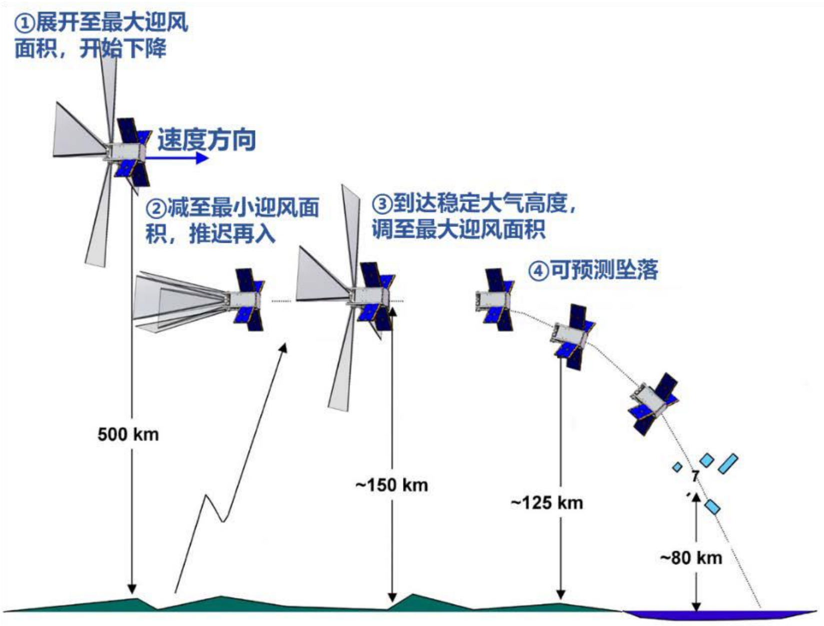

图6.1 有控再入实验

Controlled reentry experiment

本文提出了可变面质比实验任务 Cubesat 卫星的设计方案。任务可实现如图 6.1 所示的有控再入实验：卫星依靠改变迎风面与速度的夹角改变阻力大小，控制下降的轨迹。其改变迎风面积的方式，与大型航天器改变太阳能帆板的角度高度类似，因此用于实验验证气动可控再入的可操作性。本任务充分利用立方星研制和发射成本低的优势，完成了以以上可控再入试验为主要目标的任务总体设计。

In this paper, the design scheme of Cubesat satellite with variable area-to-mass ratio is presented. The mission can realize the controlled reentry experiment as shown in Figure 6.1: the satellite controls the descent trajectory by changing the angle between the windward side and the speed to change the drag. The way of changing the windward area is similar to that of changing the angle and height of solar panels in large spacecraft, so it is used to verify the operability of aerodynamic controllable reentry. This mission takes full advantage of the low cost of CubeSat development and launch, and completes the overall mission design with the above controllable reentry test as the main goal.

同时任务设计过程中充分考虑了气动帆构型被动姿态稳定的特性，并将通过实验探究不同夹角下姿态稳定的能力作为从属目标。另外，对于多变的近地轨道大气密度，任务也可以得出拟构近地轨道大气特性和变化规律的一组数据。本文从背景调研、任务分析、轨道设计、有效载荷确定和各分系统的具体设计方面阐述了整个任务的设计过程。通过航天任务分析与设计的一般流程，逐渐形成一个完整的任务设计。但是我们的任务设计还有一些亟待改进的地方，作为一个实验任务，我们对要进行的实验的阐述还不够详细。

At the same time, the characteristics of passive attitude stabilization of the aerodynamic sail configuration are fully considered in the task design process, and the ability of attitude stabilization under different angles is explored through experiments as a subordinate goal. In addition, for variable LEO atmospheric densities, the mission can also derive a set of data that mimics LEO atmospheric properties and variations. In this paper, the design process of the whole mission is described from the aspects of background investigation, mission analysis, orbit design, payload determination and specific design of each subsystem. Through the general process of space mission analysis and design, a complete mission design is gradually formed. However, there are still some areas that need to be improved in our task design. As an experimental task, our description of the experiment to be carried out is not detailed enough.

到问题、寻找解决方案、修改完善的过程中，体会真实的航天任务设计思路，理解各个组件或系统的统筹与权衡，领会分析与设计过程中反复的迭代协调解决问题的特质。

In the process of problems, finding solutions, modifying and perfecting, we can experience the real design ideas of space missions, understand the overall planning and trade-offs of various components or systems, and understand the characteristics of repeated iteration and coordination in the process of analysis and design.

我们在此向韩潮老师的指导表示感谢!

We would like to express our gratitude to Mr. Han Chao for his guidance!

参考文献
References

[1] 贾洪印,徐明兴,张培红,吴晓军,和争春.栅格翼在减小火箭残骸落点散布上的应用[J].航天返回与遥感,2018,39(06):21-29.

Jia Hongyin, Xu Mingxing, Zhang Peihong, Wu Xiaojun, He Zhengchun. Application of grid fin in reducing the impact point dispersion of rocket debris. Space Return and Remote Sensing, 2018, 39 (06): 21-29.

[2] Kristin Medlock, Kerry Nock, Kim Aaron. Gossamer Orbit Lowering Device(GOLD) for safe and efficient de-orbit[C]// AIAA/AAS Astrodynamics Specialist Conference. Washington D.C.: AIAA,2010

[3] Daan Maessen, E D Breukelen, B T C Z Bergen. Development of a generic inflatable-orbit device for Cubesats, IAC-07-A6.3.06[C]// 58th International Astronautical Congress. Paris: IAF, 2007

[4] Lappas V, Adeli N, Visagie L, et al. CubeSail: A low cost CubeSat based solar sail demonstration mission[J]. Advances in Space Research, 2011, 48(11):1890-1901

[5] Visagie L. Gossamer sails for satellite de-orbiting: Mission analysis and applications[D]. Guildford: University of Surrey, 2016

[6] Viquerat A, Schenk M, Lappas V, et al. Functional and Qualification Testing of the InflateSail Technology Demonstrator[C]//2nd AIAA Spacecraft Structures Conference.

Kissmmee:AIAA,2015:1627-1628

[7] Shmuel Barbara. Canadian advanced NanospaceXperment7(CanX-7) mission analysis, payload design and testing[D]. Toronto, Canada: University of Toronto, 2012

[8] Biddy C, Svitek T. LightSail-1 solar sail design and qualification[C]//Proceedings of the 41st Aerospace Mechanisms Symposium. Pasadena: National Aeronautics and Space Administration, 2012: 451-463.

[9] 曾玉堂. 立方体卫星制动帆离轨装置的设计与研究[D]. 南京：南京理工大学，
Zeng Yutang. Design and research of braking sail deorbit device for CubeSat [D]. Nanjing: Nanjing University of Science and Technology,

2017

[10]李诚. 立方星制动帆装置设计与应用研究[D].南京理工大学,2018.
Li Cheng. Design and application research of cubic star brake sail device [D]. Nanjing University of Science and Technology, 2018.

[11] James R. W., Wley J. L. 等, 航天任务的分析与设计[M], 王长龙 等译, 北京,航空工业出版社, 1992

James R. W., Wley J. L. Et al. Analysis and Design of Space Mission [M]. Translated by Wang Changlong et al. Beijing, Aviation Industry Press, 1992

[12] 周军, 刘莹莹, 航天器姿态与轨道控制原理[M], 西安, 西北工业大学出版社, 2016.3

Zhou Jun, Liu Yingying, Principle of Spacecraft Attitude and Orbit Control [M], Xi’an, Northwestern Polytechnical University Press, 2016.3

[13] Rawashdeh, S., et al. Aerodynamic Stability for CubeSats at ISS Orbit[J], JoSS, Vol. 2, No. 1, pp. 85-104, 2013

[14] 夏灿英, 卫星大气阻力系数的计算公式[J], 云南天文台台刊. 1982,(01)
Xia Canying. Calculation formula of atmospheric drag coefficient of satellite [J]. Bulletin of Yunnan Observatory. 1982,(01)

[15] U.S. Standard Atmosphere, 1976

[16] Нариманова Г. С., Тихонравова М. К., Основы Теории Полета Космических Аппаратов[M], Москва, Машиностроение, 1972

[17] DeOrbitSail Nanosatellite Mission, https://earth.esa.int/web/eoportal/satellite-missions/d/deorbitsail

[18] B. Banks, J. Backus, M. Manno. Atomic oxygen erosion yield prediction for spacecraft polymers in low earth orbit. International Symposium on Materials in a Space Environment (ISMSE), 2009(11)

[19] Long, A. C. and Spencer, D. A. A Scalable Drag Sail for the Deorbit of Small Satellites, JoSS ,2018 Vol. 7, No. 3, pp. 773–788